

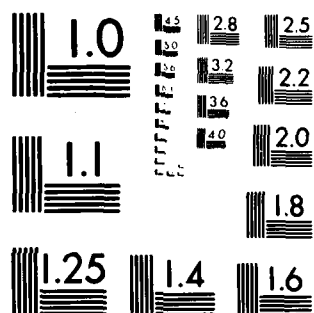
AD-A085 159

DOUGLAS AIRCRAFT CO LONG BEACH CA F/8 20/4
STUDIES ON THREE-DIMENSIONAL BOUNDARY LAYERS ON BODIES OF REVOL--ETC(U)
APR 80 T CEBEI, A A KHATTAB, K STEWARTSON N60921-78-C-0158
MDC-J8716 NL

UNCLASSIFIED

1-1
A-1000

END
DATE
FILMED
7 80
DTIC



MICROCOPY RESOLUTION TEST CHART
NATIONAL BUREAU OF STANDARDS-1963-A

ADA 085159

NAVAL SURFACE WEAPONS CENTER
CONTRACT NO. N60921-78-C-0158
FOR
NAVAL AIR SYSTEMS COMMAND
WASHINGTON D. C. 20361

This document has been approved
for public release and sale; its
distribution is unlimited.

DOUGLAS AIRCRAFT COMPANY

MCDONNELL DOUGLAS
CORPORATION

80 6 5 042

DDC FILE COPY



REPORT NO. MDC J8716

12

STUDIES ON THREE-DIMENSIONAL
BOUNDARY LAYERS ON BODIES OF REVOLUTION

II. THREE-DIMENSIONAL LAMINAR BOUNDARY
LAYERS AND THE OK OF ACCESSIBILITY

BY

TUNCER CEBECI, A. A. KHATTAB AND KEITH STEWARTSON

APRIL 1980

DTIC
ELECTE
JUN 5 1980
C

NAVAL SURFACE WEAPONS CENTER
CONTRACT NO. N60921-78-C-0158

FOR

NAVAL AIR SYSTEMS COMMAND
WASHINGTON D. C. 20361

This document has been approved
for public release and sale, in
distribution is unlimited.

SUMMARY

An investigation is carried out into the structure of the laminar boundary layer originating from the forward stagnation point of a prolate spheroid at incidence in a uniform stream, assuming that the external velocity distribution is given by attached potential theory. The principal new results of the study are:

(i) A new transformation of the body coordinates is devised which facilitates the computation of the solution near the nose,

(2) ~~(ii)~~ Two variations of the standard box method of solving the equations are devised to enable solutions to be computed in regions of cross-flow reversal. They are referred to as the zig-zag box and the characteristic box.

3) ~~(iii)~~ Whereas in two dimensional flows the effect of the boundary layer approaching separation on the external flow may be represented by a blowing velocity, in the present study we find that this is only true near the windward line of symmetry. Near the leeward line of symmetry the blowing velocity must be replaced by a suction velocity even though the boundary layer is being significantly thickened.

4) ~~(iv)~~ The boundary layer over the whole of the spheroid cannot be computed in an integration from the forward stagnation point. If $\alpha \leq 6^\circ$, the accessible region is largely bounded by the separation line and develops a wedge-like shape whose apex is named the ok of accessibility, pointing towards the nose of the spheroid. On the windward side of this line the solution develops a singularity; on the leeward side the situation is less clear but it is believed to occur there too.

5) ~~(v)~~ For $\alpha \geq 15^\circ$ the accessible region on the leeward side of the ok is largely determined by the external streamline through the ok.

$$\alpha > \alpha_R = 11.5^\circ \text{ DFG}$$

CONTENTS

	<u>Page</u>
I. INTRODUCTION	1
II. FORMULATION	9
III. THE NUMERICAL PROCEDURE	18
IV. GENERAL PROPERTIES OF THE SOLUTION	27
4.1 The Separation Line When $\alpha = 6^0$	41
4.2 The Separation Lines for $\alpha = 3^0, 15^0, 30^0$	51
V. DISCUSSION	54
VI. REFERENCES	58

Accession For	
NTIS GRA&I	
DDC TAB	
Unannounced	
Justification	
By	
Distribution/	
Availability Codes	
Dist	Available for special
A	

I. INTRODUCTION

The determination of the three-dimensional boundary layer on a body when subject to a prescribed pressure gradient has attracted much interest during the last twenty years since the general principles which must govern any sound numerical approach were laid down by Raetz (1957). These follow from the realization that the momentum equations are diffusive in the direction normal to the body and wave-like in planes parallel to the body, the direction of propagation being along the local stream direction. Since in general this direction varies across the boundary layer it is possible to identify zones of influence and of dependence for any point P of the boundary layer each being a curvilinear wedge with generators composed of normals to the body and having the normal through P as vertex line. The computation of the boundary layer properties at P must, in some sense, make use of its properties at all points in the zone of influence on P . The same remark applies to two dimensional boundary layers, the zone of dependence now reduces to a plane. The complication in three-dimensional flow is that this zone can be very broad, especially near separation where the skin-friction direction may be inclined at an obtuse angle to the main stream and even worse situations may occur. Beyond separation the zone of dependence in two dimensions is a plane extending both upstream and downstream in terms of the mainstream while in three-dimensions, it might extend in all directions, at least near P .

The concept of separation and its relation to that of accessibility is of some subtlety and requires careful consideration. The problems which can arise have been extensively studied, notably by Maskell (1955), Lighthill (1963) and Wang (1976), the last of whom also gives a well-balanced review of previous work. Accessibility is defined as follows. A point P of the boundary layer is

said to be accessible from the forward stagnation point 0 if the velocity field at P can be computed in terms of the initial conditions at 0 and the boundary conditions on the body and in the external stream. The boundary of this region consists of the normals to the body through a curve ℓ_A on the body, ℓ_A being often closed and encircling 0 but it could extend to infinity. Separation is a line ℓ_S drawn on the body which forms the boundary of all limiting streamlines emanating from 0. If ℓ_S is closed, the normals to it bound the region of accessibility but to identify ℓ_S and ℓ_A requires additional arguments, although Wang (1976) noted a general agreement that this is always the case. Later on however we shall demonstrate that important exceptions can occur.

It has been argued that ℓ_S is a limiting streamline, i.e. a skin-friction line, passing through isolated singular points of the solution (Lighthill, 1963) or is an envelope of limiting streamlines (Maskell, 1955). There is a significant difference between the nature of the boundary-layer solution according to which option occurs. For if it is an envelope, the skin friction component in a direction perpendicular to ℓ_S must have an algebraic singularity at ℓ_S with index probably equal to 1/2. Further, the displacement thickness is also singular at ℓ_S and so the solution terminates at ℓ_S . On the other hand if ℓ_S is a skin-friction line then it is possible for the solution to be smooth at ℓ_S and so may be continued beyond the region of accessibility from the forward stagnation point although, to be sure, additional information must then be supplied to specify it uniquely. Now in real flows one can reasonably expect that the pressure gradient adjusts near ℓ_S to prevent the singularity — otherwise a contradiction might well occur since the corresponding singularity in the displacement thickness provokes a singularity in the pressure gradient forcing, in turn, separation to occur earlier. This argument has already been

identified this with the free vortex-layer type of separation previously described by Maskell (1955). Another possible type of separation on smooth bodies, first identified by Howarth (1951), is a collision between two boundary layers originating from different parts of the flow field, but for a long time such a phenomenon was regarded as exceptional. Recently, however, a number of additional studies have been reported (see Stewartson, Cebeci & Chang 1980, for examples) and it seems worthwhile to bear it in mind as a possible termination of the calculations. The novel feature is that the forward calculation of the one boundary layer develops unexceptionally until it collides with the other, the exact position of the collision being determined by mechanisms which are not yet clear but which probably depend on balancing the forward momentum in each of the boundary layers.

This discussion indicates that understanding of these boundary layers, even when the pressure gradient is prescribed, is still incomplete. Our aim in this report is partly to offer an alternative numerical method which will hopefully enable us to carry the integration further towards x_s and clarify some of the outstanding issues. In addition we have some new goals.

It is well-known that in problems of engineering interest the majority of the boundary layer is turbulent, transition occurring near the nose of the body at high angles of incidence. In order to study these flows we first need an accurate method of computing the laminar flow in this neighborhood. The method used by Wang (1976) has limitations here because he does not choose to remove the singularities in the metric parameters at the nose and while the use of coordinates based on properties of the imposed mainstream formally removes them (Geissler 1975), they lead to additional difficulties [Cebeci, Kaups, Mosinskis & Rehn 1973]. Recently Cebeci, Khattab & Stewartson (1980) have devised a set of body coordinates with

extensively used in two-dimensional flows, culminating in the Sychev-Smith theory of separation on a circular cylinder and other smooth bodies (Sychev 1967, 1972, Smith 1977a, 1979), in which the flow field is regular as the skin friction changes sign. It is noted that some studies of the analogous triple-deck theory in three-dimensional flows have already been made (Burggraf 1978, Smith, Sykes and Brighton 1977, Sykes 1979) and the flow near separation is again regular. Now there are many photographs available of three-dimensional separation; Wang (1976) has included a selection in his review, for example, and Han and Patel (1979) have published some for laminar flows past spheroids. These strongly suggest that λ_s is an envelope, but for the above reason we are reluctant to accept that this is really the case and are of the opinion that a more detailed study would show it to be a skin-friction line as Lighthill suggested.

There have been a number of careful calculations of three-dimensional boundary layers in the past particularly by Wang (1970, 1974a,b,c, 1972, 1975) and by Cebeci and his associates (1973, 1976), but for all the computation of the separation line λ_s has proved difficult, if not impossible. The most successful are due to Wang for boundary layers on a prolate spheroid at incidence; but even he was not able to comment usefully on the nature of the solution near separation, and the computation on the leeward side of the body proved very difficult. He took careful note of the zones of dependence in formulating his numerical algorithm and used an implicit finite-difference method based on the Crank-Nicholson scheme. For an angle of attack $\alpha = 30^\circ$ he concluded that the closed separation line λ_s , which we have already discussed at length, is replaced by an open separation line λ_o , which starts about 10% of the way to the back of the body and about 140° from the windward line of symmetry, the limiting streamlines approaching it from both sides. He

respect to which the governing equations are regular everywhere upstream of x_A . Here we shall use this system of coordinates and, indeed, make a further transformation to convert the formal computation of the flow near the nose into a straightforward numerical problem, so that we shall later be in a strong position to examine the stability of the laminar boundary layer.

Second we wish to have a method easily adaptable to the integration of turbulent boundary layers. For such flows it is known that a variable mesh normal to the body is desirable, to cope with this characteristic double-structured form. A generalization of the Cebeci-Smith eddy-viscosity model (Cebeci & Bradshaw 1977) has quite good prospects for providing an adequate description of such flows and the corresponding equations have close similarities to those for laminar flow. This requirement can be met by using the Keller-box method (Cebeci & Bradshaw 1977) in which the governing equations are reduced to five first-order finite-difference equations in terms of values either at the corners or the centers of the sides of the box to give a second-order accurate solution at the center of the box. These boxes are now stacked one on top of the other with one set of edges along the normals to the surface. The nonlinear difference equations are linearized by using Newton's method and then solved by a standard procedure to give the values of the five dependent variables on the fourth normal in terms of the other three. In this way the solution can be advanced from either the windward or leeward line of symmetry, where it can be found independently downstream from the nose. We shall refer to this method as the standard box.

A deficiency in the standard box is that it ignores Raetz's principle of the zone of dependence and so the user is not surprised that it eventually breaks down as separation is approached and particularly after the circumferential skin-friction has changed sign. Two modifications are then brought into use.

First Krause et al. (1968) suggested that a zig-zag scheme might be helpful in this situation: in an integration advancing from the windward line of symmetry this amounts to replacing one of the edges of the box on the upstream (and known) side by the next edge further to leeward. We investigate its usefulness here, referring to the modification as the zig-zag box, first used by Cebeci (1979) for unsteady flows.

However this approach does not entirely mimic the wave-like character of the momentum equations. For this the box should be replaced more appropriately by a curvilinear surface consisting of the (projections of the) streamlines on planes parallel to the surface passing through the normal edge along which we wish to compute the values of the dependent variables. For this purpose we use a new numerical algorithm developed by Cebeci and Stewartson (1977), which incorporates this requirement: we shall refer to it subsequently as the characteristic box, thus acknowledging that the streamlines are characteristics of the momentum equations.

With these schemes at our disposal we integrate the boundary-layer equations for a prolate spheroid for a thickness ratio $t = 1/4$, set at an angle of incidence α to an oncoming stream where $\alpha = 3^\circ, 6^\circ, 15^\circ, 30^\circ$, taking the imposed pressure gradient to be that given by classical potential theory. In parenthesis we note that the experimental pressure variations agree closely with this theory except, significantly, near separation (Patel & Choi 1979), (Meier & Kreplin 1979). We find no difficulty in determining the solution near the nose and up to the line of cross-skin friction reversal using the standard box. Further downstream, both the zig-zag box and the characteristic box were used and both found to be effective, particularly on the leeward side, where there is an extended region before separation occurs; it appears that the characteristic box is the more accurate and so in the final presentation of results it is preferred.

The most complete of the earlier studies of the flow fields is for $\alpha = 6^\circ$, due to Wang (1975), who concludes that it may be computed as far as the separation line ℓ_s , which has the shape of a tongue half-way between the windward line of symmetry ℓ_w and the leeward ℓ and extends significantly towards the nose. Our results indicate the same general trends, but the tongue is much more pronounced and takes on a wedge-like character, which we shall refer to as an ok (lit. arrow, Turk.). The boundary of the region of accessibility, defined by the curve ℓ_A , thus largely coincides with ℓ_s when $\alpha = 6^\circ$. In addition we are able to carry the computation near enough to this line on the windward side to provide convincing evidence that the solution develops a singularity there, probably of the type described by Brown (1965). In contrast to Wang's results we find that the circumferential skin-friction does not vanish on ℓ_s , and nor does the tangential component along ℓ_s . On the leeward side we find marked quantitative differences in the magnitude of the skin friction near ℓ_s and indeed in the position of ℓ_s . However, the leeward portion of ℓ_s cannot be fixed so definitely as the windward side since we are unable to reproduce the Brown singularity at all; nevertheless we are fairly confident that the position of ℓ_s inferred from our computations is close to being correct.

At $\alpha = 15^\circ$ the identification between ℓ_A and ℓ_s is only possible on the windward side. The form of ℓ_s is similar to that for $\alpha = 6^\circ$ except that it originates at $\xi \doteq -0.4$ and in particular the solution is clearly singular there. On the leeward side, however, ℓ_A is determined by the external streamline passing above the most forward point of the windward separation line. The reason is that downstream of this line the solution in the outer part of the boundary layer is historically dependent on flow properties along streamlines which have passed over the windward line of

separation and these properties are not fully known. Thus an ok forms in ϵ_A also when $\alpha = 15^\circ$, but for a different reason, and now there is no possibility of an accurate determination of the leeside shape of ϵ_s with the boundary values and initial conditions supplied. In fact the concept of separation is strictly meaningless here and the notion of open separation introduced by Wang (1975) is irrelevant, although no doubt important in many practical flows. Similar remarks apply to the solution when $\alpha = 30^\circ$.

An important aspect of the boundary layer is the role it plays in correcting the external velocity. In two-dimensional studies, this may be interpreted as an injection velocity from the body into the inviscid stream, especially near separation. The corresponding result for the three-dimensional boundary layers under investigation here is the same over the majority of the flow field computed, but near ϵ beyond the reversal of circumferential velocity the injection velocity is replaced by a suction velocity. Although this unexpected result may easily be inferred from previous studies, it does not seem to have been noted. There is a tendency for the boundary layer to thicken in this region but nevertheless its effect on this equivalent injection velocity is the opposite to that expected.

II. FORMULATION

The studies in this paper extend those of Cebeci et al. (1980) and we shall largely follow their notation and formulation. The governing boundary-layer equations for an incompressible laminar flow in a curvilinear orthogonal coordinate system appropriate to a prolate spheroid at incidence (Fig. 1) are

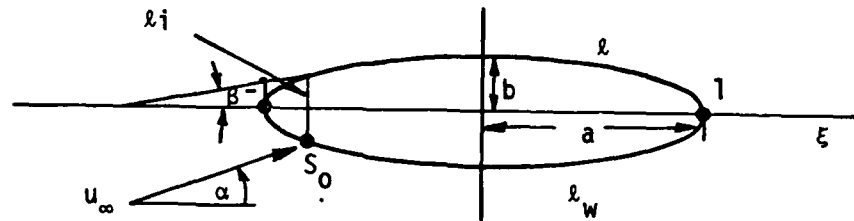


Figure 1. Notation for prolate spheroid at incidence.

Continuity

$$\frac{\partial}{\partial x} (h_2 u) + \frac{\partial}{\partial \theta} (h_1 w) + \frac{\partial}{\partial y} (h_1 h_2 v) = 0 \quad (2.1)$$

x-Momentum

$$\frac{u}{h_1} \frac{\partial u}{\partial x} + \frac{w}{ah_2} \frac{\partial u}{\partial \theta} + v \frac{\partial u}{\partial y} + \frac{w^2 K_2}{a} = -\frac{1}{\rho h_1} \frac{\partial p}{\partial x} + \nu \frac{\partial^2 u}{\partial y^2} \quad (2.2)$$

θ -Momentum

$$\frac{u}{h_1} \frac{\partial w}{\partial x} + \frac{w}{ah_2} \frac{\partial w}{\partial \theta} + v \frac{\partial w}{\partial y} - \frac{uwK_2}{a} = -\frac{1}{\rho ah_2} \frac{\partial p}{\partial \theta} + \nu \frac{\partial^2 w}{\partial y^2} \quad (2.3)$$

where (u, w) are the velocity components parallel to the body surface and in, respectively, the meridional and azimuthal directions, while v is the component normal to this surface. Further h_1, h_2 are metric coefficients, where h_1 and h_2 are defined by

$$h_1 = \left[\frac{1 + \xi^2(t^2 - 1)}{1 - \xi^2} \right]^{1/2}, \quad h_2 = t(1 - \xi^2)^{1/2}, \quad (2.4)$$

t denotes the thickness ratio ($=b/a$) of the elliptic profile and $\xi = x/a$. The parameter K_2/a is the geodesic curvature of the surface lines $\xi = \text{const.}$ with K_2 given by

$$K_2 = \frac{t\xi}{h_1 h_2 (1 - \xi^2)^{1/2}} \quad (2.5)$$

The solution of the system (2.1) to (2.5) requires boundary conditions and initial conditions. The boundary conditions are:

$$\begin{aligned} y = 0, & \quad u = v = w = 0, \\ y \rightarrow \infty, & \quad u \rightarrow u_e(x, \theta), \quad w \rightarrow w_e(x, \theta) \end{aligned} \quad (2.6)$$

The velocity components u_e and w_e can be obtained from inviscid theory, (Hirsh and Cebeci 1977), being given by

$$\frac{u_e}{u_\infty} = V_0(t) \cos \alpha \cos \beta - V_{90}(t) \sin \alpha \sin \beta \cos \theta \quad (2.7a)$$

$$\frac{w_e}{u_\infty} = V_{90}(t) \sin \alpha \sin \theta. \quad (2.7b)$$

Here β denotes the angle between the line tangent to the elliptic profile and the positive ξ -axis: it is given by

$$\cos \beta = \frac{(1 - \xi^2)^{1/2}}{[1 + \xi^2(t^2 - 1)]^{1/2}} \quad (2.8)$$

The parameters $V_0(t)$ and $V_{90}(t)$ are functions of t , defined by

$$V_0(t) = \frac{(1 - t^2)^{3/2}}{\sqrt{(1 - t^2)} - \frac{t^2}{2} \ln \left\{ \frac{[1 + (1 - t^2)^{1/2}]}{[1 - (1 - t^2)^{1/2}]} \right\}} \quad (2.9a)$$

$$V_{90}(t) = \frac{2V_0(t)}{2V_0(t) - 1} \quad (2.9b)$$

As formulated, the governing equations are singular at the nose ($\xi = -1$) and this may be removed, as explained in Cebeci et al (1980), by the following transformation. We define new velocity components U, W, V by

$$u = U \cos \theta + W \sin \theta, \quad w = W \cos \theta - U \sin \theta, \quad tv = V \quad (2.10)$$

and new coordinates X, Y, Z by

$$X = S \cos \theta, \quad Z = S \sin \theta, \quad tY = y \quad (2.11)$$

where

$$\frac{dS}{S} = \left[\frac{[1 + \xi^2(t^2 - 1)]}{t(1 - \xi^2)} \right]^{1/2} d\xi = \frac{h_1 dx}{h_2} \quad (2.12)$$

Then (2.1) to (2.3) reduce to

$$N \left(\frac{\partial U}{\partial X} + \frac{\partial W}{\partial Z} \right) + \frac{\partial V}{\partial Y} - L(UX + WZ) = 0, \quad (2.13)$$

$$N \left(U \frac{\partial U}{\partial X} + W \frac{\partial U}{\partial Z} \right) + LW(WX - UZ) + V \frac{\partial U}{\partial Y} = \tilde{\beta}_1 + v \frac{\partial^2 U}{\partial Y^2}, \quad (2.14)$$

$$N \left(U \frac{\partial W}{\partial X} + W \frac{\partial W}{\partial Z} \right) - LU(WX - UZ) + V \frac{\partial W}{\partial Y} = \tilde{\beta}_2 + v \frac{\partial^2 W}{\partial Y^2}, \quad (2.15)$$

where $\tilde{\beta}_1$ and $\tilde{\beta}_2$ are pressure-gradient parameters defined by

$$\tilde{\beta}_1 = N \left(U_e \frac{\partial U_e}{\partial X} + W_e \frac{\partial U_e}{\partial Z} \right) + L W_e (W_e X - U_e Z), \quad (2.16a)$$

$$\tilde{\beta}_2 = N \left(U_e \frac{\partial W_e}{\partial X} + W_e \frac{\partial W_e}{\partial Z} \right) - L U_e (W_e X - U_e Z) \quad (2.16b)$$

and

$$N = \frac{St^2}{h_2}, \quad L = \frac{t^2}{S} \left(\frac{1}{h_2} + K_2 \right). \quad (2.17)$$

This new set of equations (2.10) to (2.17) is free of any singularities at the nose and moreover takes a well-behaved form as $t \rightarrow 0$; thus they are formally well-suited to initiate the computation on thin prolate spheroids, or indeed any other shapes provided they have paraboloidal noses. The corresponding boundary conditions are

$$u = v = w = U = V = W = 0 \quad \text{when } y = Y = 0 \quad (2.18a)$$

and

$$u \rightarrow u_e, \quad w \rightarrow w_e, \quad U \rightarrow U_e, \quad W \rightarrow W_\infty \quad \text{as } y, Y \rightarrow \infty \quad (2.18b)$$

where u_e, w_e, U_e, W_e are related by formulas equivalent to (2.10). Initial conditions are also imposed at the stagnation point S_0 , defined from (2.7) by

$$\theta = 0, \quad \xi = -V_0(t) [V_0^2(t) + t^2 V_{90}^2(t) \tan^2 \alpha]^{1/2} \equiv \xi_0, \quad (2.19)$$

$$\text{and are} \quad U = W = 0, \quad Y \geq 0. \quad (2.20)$$

In the neighborhood of this point, which we define to be $(X_0, 0)$ in the (X, Z) coordinate system we may write

$$U = (X - X_0) \hat{U}(Y), \quad W = Z \hat{W}(Y), \quad V = \hat{V}(Y) \quad (2.21)$$

and then \hat{U}, \hat{W} satisfy

$$N\hat{U}^2 + V \frac{d\hat{U}}{dy} = \beta_1^{**} + v \frac{d^2\hat{U}}{dy^2}, \quad N\hat{W}^2 + V \frac{d\hat{W}}{dy} = \beta_2^{**} + v \frac{d^2\hat{W}}{dy^2} \quad (2.22)$$

$$N(\hat{U} + \hat{W}) + \frac{dV}{dy} = 0,$$

where

$$\beta_1^{**} = N \left(\frac{\partial U}{\partial X} e \right)^2, \quad \beta_2^{**} = N \left(\frac{\partial W}{\partial Z} e \right)^2 \quad (2.23)$$

are evaluated at $(X_0, 0)$. These stagnation flow equations are a special case of Howarth's equations (1951).

While it is true that one may now proceed to solve this new form of the three-dimensional boundary layer equations from the forward stagnation point past the nose and as far downstream as x_A , there are still some awkward features about initiating the calculations; these may be avoided by means of yet another transformation. Since the final form of the equations is so convenient for the computer it was decided to make use of them in spite of the slightly more complicated algebraic structure. The strategy underlying our thinking is as follows. The standard-box method depends for its success on knowing the solution on three of the four normals in which the boxes are stacked at each stage. In the formulation (2.10) - (2.17) we can determine the

solution on $Z = 0$ (Cebeci et al 1980, Wang 1970), but how can we find the solution on the first normal of the first station, say $X = 0$, $Z = k$, off the windward line of symmetry? Of course, once we have this, the standard box is well suited to finding the solution at all the normals standing on the line $Z = k$, but a special method is needed to get the first solution. However, since we have the solution on the line of symmetry we could use this provided we changed to polar coordinates (R^*, ϕ^*) centered at S_0 and advanced the solution from $R^* = 0$ using the box method to carry us from $\phi^* = 0$ to $\phi^* = \pi$ at each new station of R^* . There is another point. Once we get away from the neighborhood of the nose the disadvantages of the original system (2.1) - (2.6) disappear and its simplicity both in formulation and geometric interpretation are compelling reasons for basing our solution on it. Thus we need a transformation which converts the polar coordinates centered at S_0 to the 'polar coordinates' $(\xi+1, \theta)$ centered at the nose within an acceptably small distance from it.

There are many ways of achieving these aims and we choose here to use the theory of coaxial circles. We write

$$X = X_0 + (n^2 - 1) X_0 R(R + \cos\phi)\Delta, \quad Z = (n^2 - 1) X_0 R\Delta \sin\phi \quad (2.24a)$$

$$\text{where} \quad \Delta = (1 + 2R \cos\phi + R^2)^{-1} \quad (2.24b)$$

and $n(>1)$ is an arbitrary parameter; later on we shall set $n = 2$. Other values of n may well be more convenient in special circumstances. Then when $R \ll 1$

$$X = X_0 + X_0(n^2 - 1) R \cos\phi + O(R^2), \quad Z = X_0(n^2 - 1) R \sin\phi + O(R^2), \quad (2.25)$$

so that R, ϕ are polar coordinates based on S_0 , while when $R = n^{-1}$

$$X = n X_0 \cos \theta, \quad Z = n X_0 \sin \theta, \quad (2.26)$$

where

$$\tan \theta / 2 = \frac{(n-1)}{n+1} \tan \phi / 2,$$

which returns us to the coordinate system of (2.1) - (2.6). Henceforth we shall take $n = 2$ but the generalization to arbitrary n is quite straightforward.

Define

$$U = RQ(R, \phi)Q(R, \phi, Y) \{ \cos \phi (1+R^2) + 2R \} \Delta - RT(R, \phi)T(R, \phi, Y)(1-R^2) \sin^2 \phi \Delta \quad (2.27a)$$

and

$$W = R\Delta(1-R^2) \sin \phi Q + R\Delta[\cos \phi (1+R^2) + 2R] T \sin \phi, \quad (2.27b)$$

so that when $R = 1/2$, Q and $T \sin \phi$ may be identified with u and w .

Then the equations satisfied by Q, T, V are

(a) Continuity

$$\begin{aligned} \frac{N(S)}{3X_0\Delta} \left[R \frac{\partial Q}{\partial R} + \sin \phi \frac{\partial T}{\partial \phi} + \Delta[\cos \phi (1+R^2) + 2R]T + 2\Delta Q(1 + R \cos \phi) \right] \\ + \frac{\partial V}{\partial Y} - L(S) [UX + \sin^2 \phi \hat{W}\hat{Z}] = 0 \end{aligned} \quad (2.28)$$

(b) R-Momentum

$$\begin{aligned} \frac{N(S)}{3X_0\Delta} \left[RQ \frac{\partial Q}{\partial R} + \sin \phi T \frac{\partial Q}{\partial R} + Q^2 + 2R \Delta \sin^2 \phi QT - (1-R^2)\Delta \sin^2 \phi T^2 \right] \\ + L(S) \sin^2 \phi T(\hat{W}\hat{X} - U\hat{Z}) + V \frac{\partial Q}{\partial Y} = v \frac{\partial^2 Q}{\partial Y^2} + \beta_R^* (R, \phi) \end{aligned} \quad (2.29)$$

(c) ϕ -Momentum

$$\frac{N(S)}{3X_0\Delta} \left[RQ \frac{\partial T}{\partial R} + \sin\phi T \frac{\partial T}{\partial \phi} + \cos\phi T^2 + 2\Delta(1+R \cos\phi)QT - 2\Delta RQ^2 \right] - L(S) Q(\hat{W}X - U\hat{Z}) + V \frac{\partial T}{\partial Y} = v \frac{\partial^2 T}{\partial Y^2} + \beta_\phi^* (R, \phi). \quad (2.30)$$

Here

$$\hat{W} \sin\phi = W \quad \text{and} \quad Z = \hat{Z} \sin\phi \quad (2.31)$$

and β_R^*, β_ϕ^* are pressure gradient terms, not reproduced here, but which may easily be written down in terms of the main stream values Q_e, T_e of Q, T and these follow at once from the values of U_e, W_e using (2.27). The point of the relationship in (2.31) is that now the lines-of-symmetry equations can be written down at once from (2.28) - (2.30) on setting $\phi = 0, \pi$ and remembering that \hat{W}, \hat{Z} are finite. Thus the values of Q, T on $\phi = 0, \pi$ can be computed separately, and in essence have been (Cebeci et al, 1980), independently of the solution in $0 < \phi < \pi$. Further, Q and T are known at $R = 0$ for $0 < \phi < \pi$ from the solution of the stagnation equations (2.21) - (2.23):

$$\begin{aligned} Q(0, \phi, Y) &= 3X_0 [\hat{W}(Y) \sin^2\phi - \hat{U}(Y) \cos^2\phi] \\ T(0, \phi, Y) &= 3X_0 \cos\phi [\hat{U}(Y) + \hat{W}(Y)] \end{aligned} \quad (2.32)$$

When we couple known solutions at $R = 0$, and $0 < \phi < \pi$, $\phi = 0$ and $R > 0$, $\phi = \pi$ and $R > 0$, with the boundary conditions at $y = 0$ and as $y \rightarrow \infty$, it is clear that in spite of the more complicated form of (2.28) - (2.30) a numerically attractive formulation of the original problem has been achieved. We may now use the box method to compute the solution systematically along lines of constant R starting from $R = 0$ and increasing ϕ from 0 to π at each new station of R . Further the new form of the equations is well-suited for the numerical schemes proposed by Wang (1974, 1975).

Before embarking on the numerical solution it is convenient to remove u_∞ , v from the equations by making appropriate scale transformations, but to save further complications in notation we shall simply set $u_\infty = v = 1$ from now on.

III. THE NUMERICAL PROCEDURE

The standard box method for solving the governing equations may be illustrated by considering them in their original form, which we use for calculating the flow field when $S > 2X_0$ or, more strictly, its equivalent in terms of ξ , conveniently defined as $\xi > \hat{\xi}$.

Difficulties can arise with this formulation when α is small because the convenient step length in terms of η is much larger than that in terms of Y used when $\xi < \hat{\xi}$. To avoid this problem Y may be used as variable until say $\xi = 0$ when a further switch to η could be made.

The equations are reorganized by writing

$$\eta = y/s^{1/2}, \quad s = \int_{-1}^{\xi} h_1 d\xi \quad (3.1)$$

and with primes denoting differentiation with respect to η ,

$$u(\xi, y, \theta) = f(\xi, \eta, \theta), \quad w(\xi, y, \theta) = g(\xi, \eta, \theta) \quad (3.2a)$$

$$f' = p(\xi, \eta, \theta), \quad g' = q(\xi, \eta, \theta) \quad (3.2b)$$

$$e' = \frac{1}{h_1} \frac{\partial f}{\partial \xi} + \frac{1}{h_2} \frac{\partial g}{\partial \theta} + f \left(\frac{1}{2s_1} - K_2 \right). \quad (3.2c)$$

The equation of continuity may now be integrated to give

$$v = \sqrt{s} \left(\frac{1}{2s} \eta f - e \right) \quad (3.2d)$$

and the momentum equations reduce to

$$p' + s\beta_1 + spe - sK_2 g^2 = s \left(\frac{f}{h_1} \frac{\partial f}{\partial \xi} + \frac{g}{h_2} \frac{\partial f}{\partial \theta} \right) \quad (3.2e)$$

$$q' + s\beta_2 + sqe + sK_2 fg = s \left(\frac{f}{h_1} \frac{\partial q}{\partial \xi} + \frac{g}{h_2} \frac{\partial q}{\partial \theta} \right) \quad (3.2f)$$

where β_1, β_2 are dimensionless pressure gradient parameters with the property that (3.2e), (3.2f) are automatically satisfied in the limit $\eta \rightarrow \infty$ when

$$f \rightarrow u_e, \quad g \rightarrow w_e, \quad p \rightarrow 0, \quad q \rightarrow 0. \quad (3.3a)$$

The additional boundary conditions are that

$$f = g = e = 0 \quad \text{at} \quad \eta = 0 \quad (3.3b)$$

A three-dimensional grid is now set up in the (ξ, θ, η) space consisting of straight lines in the ξ, θ, η directions dividing up the domain of integration into a set of boxes. Let us conveniently label a particular box by (i, j, k) where the box $(1, 1, 1)$ has three sides on the initial planes $\xi = \hat{\xi}$, $\eta = 0$ and $\theta = 0$ respectively. Further let the ξ coordinates of the corners of the (i, j, k) box be ξ_i, ξ_{i-1} where $\xi_i - \xi_{i-1} = r_i$, the η coordinates be η_j, η_{j-1} where $\eta_j - \eta_{j-1} = h_j$ and the θ coordinates θ_n, θ_{n-1} where $\theta_n - \theta_{n-1} = k_n$ (see Fig. 2 for a typical box). It is noted that there is no need for any equality between any of the

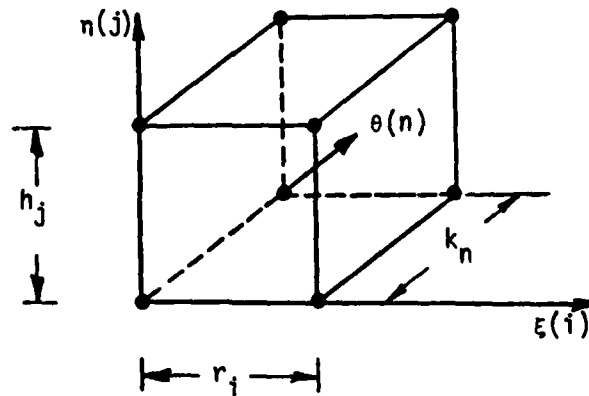


Figure 2. Finite difference molecule for the standard box.

different r_i, h_j, k_n . We now suppose that f, g, p, q are known at the mesh points $(\xi_{i-1}, \eta_j, \theta_{n-1}), (\xi_{i-1}, \eta_j, \theta_n), (\xi_i, \eta_j, \theta_{n-1})$ for all j and wish to compute them at the mesh points $(\xi_i, \eta_j, \theta_n)$. The difference approximations to (3.2b,c,e,f) are written in a standard form (see for example Cebeci & Bradshaw 1977) which may be briefly described as follows. Equations (3.2b) are approximated using centered difference-quotients and averages about the mid point $(\xi_i, \eta_{j-\frac{1}{2}}, \theta_n)$, $\eta_{j-\frac{1}{2}} = (\eta_{j-1} + \eta_j)$. The difference equations which are to approximate (3.2c,e,f) are written about the mid-point $(\xi_{j-\frac{1}{2}}, \eta_{j-\frac{1}{2}}, \theta_{k-\frac{1}{2}})$ of the cube. In centering the parameters f, g, p, q at this point we use formulas of the type

$$\bar{f}_{j-\frac{1}{2}} = \frac{1}{2} (\bar{f}_j + \bar{f}_{j-1}), \quad \bar{f}_j = \frac{1}{4} (f_j^{i,n} + f_j^{i-1,n} + f_j^{i,n-1} + f_j^{i-1,n-1}) \quad (3.4)$$

thus ascribing equal weight to the values of f at all corners of the box. The centering of the fifth parameter e proceeds differently. We do not tabulate it at the corners of the box but instead at the mid-points of the sides $n = \text{constant}$. Thus by analogy with (3.4) we treat \bar{e}_j as unknown and define

$$\bar{e}_{j-\frac{1}{2}} = \frac{1}{2} (\bar{e}_j + \bar{e}_{j-1}). \quad (3.5)$$

If at any stage of the computation we require e on the mesh points, we must interpolate among the tabulated values. This special treatment for e is necessary to avoid unacceptable oscillations. The derivatives in (3.2c,e,f) are approximated by formulas such as

$$f' = \frac{1}{h_j} (\bar{f}_j - \bar{f}_{j-1})$$

$$\begin{aligned} \frac{\partial f}{\partial \xi} = \frac{1}{4r_i} & \left[f_j^{i,n} - f_j^{i-1,n} + f_j^{i,n-1} - f_j^{i-1,n-1} + f_{j-1}^{i,n} - f_{j-1}^{i-1,n} \right. \\ & \left. + f_{j-1}^{i,n-1} - f_{j-1}^{i-1,n-1} \right] \end{aligned} \quad (3.6)$$

The difference equations together with the boundary condition (3.3) form a non-linear algebraic system for the unknown quantities $f_j^{i,n}$, $g_j^{i,n}$, $p_j^{i,n}$, $q_j^{i,n}$, \bar{e}_j (all j) which we linearize by Newton's method and solve the resulting linear system using the block-elimination method discussed in Cebeci and Bradshaw (1977). In order to start the computation, the values of f, g, p, q but not e are required on the planes $\theta = 0$ and $\xi = \hat{\xi}$. These are provided by the windward line of symmetry solution already obtained as a separate and self-contained computation and by the computation for the nose region. In turn the nose region can also be solved by the standard box provided we use the third formulation of the equations (2.30)-(3.2) and is initiated by the stagnation-point solution (3.3). Thus we have a viable numerical procedure for the integration of the boundary layer equations which we may use until it breaks down due to loss of convergence of the iteration sequence.

The seeds for this possibility are sown in the arbitrary assumption that the integration must proceed in the directions of ξ increasing and of θ increasing. We note in parenthesis that the integration could equally well proceed in the direction of θ decreasing, starting from the leeward line of integration since the solution there can and has also been computed separately (Cebeci et al 1980), but this does not overcome the fundamental weakness of the standard box. For the evolution of the boundary layer proceeds, as explained earlier, by diffusion in the η direction and by convection along

the local streamline direction, at the value of η being considered. So long as this direction is roughly the same as that of the mainstream and in particular both ξ and θ are increasing along this streamline, the standard box should be an acceptable procedure; the main feature that must be checked is that all the local streamlines from points on the lines $\xi = \xi_i, \theta = \theta_n$ cross the plane $\xi = \xi_{i-1}$ at points inside the boxes. If not, the zone of influence on this line extends outside the stacked boxes but this physical solution is easily removed by decreasing the values of r_i, k_n .

Suppose however the local streamline at $\eta = \eta_j$ is in the direction of θ decreasing while that of the external flow is in the direction of θ increasing. No adjustment of mesh lengths can remove the unphysical features of the standard box and a radical change is necessary. We have investigated two possibilities. The first is a development of the zig-zag difference scheme first used by Cebeci (1979) for unsteady flows and which we shall refer to as the zig-zag box.

In this scheme we retain the same procedure for solving (3.2b). Suppose for definiteness we have started the computation on the windward line of symmetry. Then for the other equations we modify the algebraic difference equations only if $g_{i-\frac{1}{2}}^{i,n} < 0$. We write (3.2c,e,f) as algebraic equations centered at P, using quantities centered at P,Q,R where

$$P = (\xi_{i-\frac{1}{2}}, \eta_{j-\frac{1}{2}}, \theta_n), \quad Q = (\xi_i, \eta_{j-\frac{1}{2}}, \theta_{n-\frac{1}{2}}), \quad R = (\xi_{i-1}, \eta_{j-\frac{1}{2}}, \theta_{n-\frac{1}{2}}) \quad (3.7)$$

On the other hand if the integration starts from $\theta = \pi$ then the standard box is abandoned locally only if $g_{j-\frac{1}{2}}^{i,n} > 0$. The first situation occurs near the surface $\eta = 0$ and the second in the outer part of the boundary layer.

The pattern of the zig-zag scheme in each case may be seen from Fig 3 which shows a section of the grid by the plane $\eta = \eta_{j-\frac{1}{2}}$

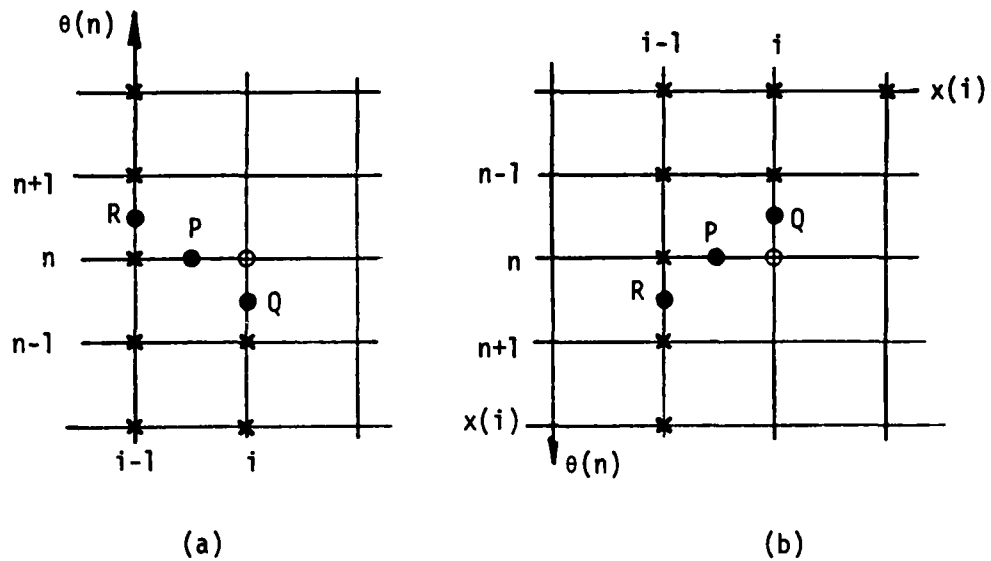


Figure 3. Finite-difference molecule for the zig-zag box when the solution procedure begins from (a) the windward plane, and (b) the leeward plane. In each case x denotes known values and o computed by the zig-zag box.

To illustrate the centering of the equations with this zig-zag box let us consider a model equation for (3.2e)

$$p' + spe = s \frac{f}{h_1^*} \frac{\partial f}{\partial \xi} + \frac{g}{h_2^*} \frac{\partial f}{\partial \theta} \quad (3.8)$$

where we have temporarily added stars to the metric functions to prevent confusion with the step-length in the n direction. The finite difference approximations to this equation for the case when the marching in the θ direction is from windward to leeward are (Fig (3b)):

$$p'(P) + (spe)(P) = \frac{s}{h_1^*} (P) f(P) \frac{\partial f}{\partial \xi} (P) + \frac{s}{h_2^*} (P) \left[\gamma_n g(Q) \frac{\partial f}{\partial \theta} (Q) + (1 - \gamma_n) g(R) \frac{\partial f}{\partial \theta} (R) \right] \quad (3.9)$$

Here the capital letter following each group of numerical quantities indicates the point at which they are to be centered and for this purpose we use the neighboring mesh points of ξ for P and neighboring mesh points of θ for Q and R. Additionally

$$\gamma_n = \frac{\theta_{n+1} - \theta_n}{\theta_{n+1} - \theta_{n-1}} \quad (3.10)$$

Again we have an algebraic system of equations for finding the values of the dependent variables at $(\xi_i, \eta_j, \theta_n)$ (all j) which is solved by the procedure followed in the standard box scheme. A variation of this method has been successfully applied to the computation of unsteady laminar boundary layers (Cebeci 1979) and we shall make use of it here when the cross-flow velocity g changes sign across the layer.

Although the zig-zag box is a definite improvement on the standard box it still contains some physical weaknesses. Thus for the determination of p from (40) at $(\xi_i, \eta_j, \theta_n)$ the values of f, g, p, q at $(\xi_i, \eta_j, \theta_{n+1})$ are not directly relevant since distributions are being carried forward along the local streamline. Of crucial importance in fact are the values of f, g, p, q, at $(\xi_{i-1}, \eta_j, \theta)$, this being the point in the plane $\xi = \xi_{i-1}$ where it intersects the projection of the streamline through $(\xi_i, \eta_j, \theta_n)$ on the plane $\eta = \eta_j$.

Following the same line of argument the attaching of equal weights to the centered mesh points on either side of R does not allow for the possibility that if this streamline passes close to one of them the other may almost be discounted. For this reason we use a third form of the Keller-box method which incorporates these physical arguments and which we shall refer to as the characteristic box (see Fig. 4). The method, developed by Cebeci and Stewartson (1977), is usually used for all j when $g < 0$ for any j in the calculations

starting from the windward side (and vice versa from the leeward side) but it can be applied even if $g \geq 0$ for all j . The standard procedure is retained for (3.2b) and the zig-zag procedure for the continuity equation (3.2c). In order to obtain the difference approximations to (3.2e,f) we first write them in streamline form, that is:

$$p' + s\beta_1 + spe - sK_2g^2 = \Lambda \frac{\partial f}{\partial \psi} \quad (3.10a)$$

$$q' + s\beta_2 + sqe + sK_2fg = \Lambda \frac{\partial g}{\partial \psi} \quad (3.10b)$$

where ψ is measured along the projection of the local streamline in the plane $\eta = \text{const}$ and

$$\Lambda = s \left[(f/h_1^*)^2 + (g/h_2^*)^2 \right]^{1/2}. \quad (3.11)$$

The value of θ is found by drawing a straight line through $(\xi_i, \eta_j, \theta_k)$ in a direction equal to the mean of the streamline directions at $(\xi_{i-1}, \eta_j, \theta)$ and $(\xi_i, \eta_j, \theta_k)$. This necessitates an additional measure of iteration in the numerical scheme. The values of the relevant variables at $(\xi_{i-1}, \eta_j, \theta)$ are found by quadratic interpolation between the known values at $(\xi_{i-1}, \eta_j, \theta_{n-1})$, $(\xi_{i-1}, \eta_j, \theta_n)$ and $(\xi_{i-1}, \eta_j, \theta_{n+1})$. The equations (43) are then differenced at the mid point ϕ between $(\xi_i, \eta_j, \theta_k)$ and $(\xi_{i-1}, \eta_j, \theta)$ (see Fig.4), and finally the value of e at ϕ is found by linear interpolation from its value at P , where equations to find it already have been written down, and the values of e at smaller values of k . It is believed that the errors involved in this procedure are second order, i.e. the same as those in the standard box method. The method has already been used effectively in a study of laminar and turbulent boundary layers on ship hulls (Cebeci, Chang, and Kaups 1978) as well as three-dimensional flows on wings.

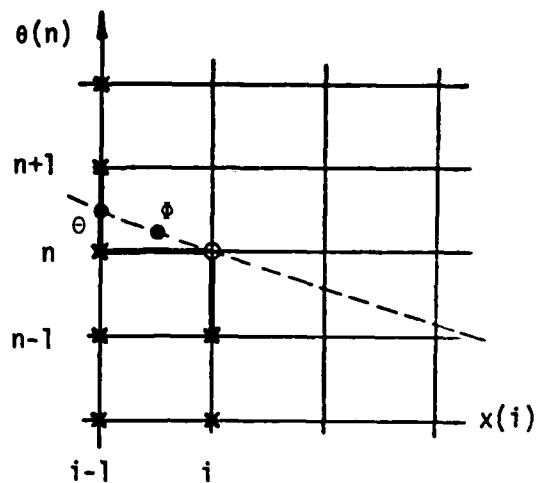


Figure 4. Finite-difference pattern for the characteristic box. The heavy lines show the pattern for the zig-zag scheme for continuity equation, x denotes known quantities and o those to be computed by the characteristic box.

The characteristic box may also be used to extend the solution in the nose region away from the line of symmetry in the second form of the equations, (2.13) - (2.15). Here the solution is known on $Z = 0$ and it enables us to deduce the solution at ψ , the first X-station of the first grid lines adjacent to those at $Z = 0$. The computation of e at ψ is effected by extrapolation from P using its symmetry properties on $Z = 0$. Having computed the solution at this station of X those at other stations of X follow using the standard box. The process is repeated at each of the Z grid lines.

The characteristic box is complicated and requires a little more programming effort than either the standard or the zig-zag boxes but it has a greater range of applicability than they or, we believe, any other method available at present. However it does have limits; thus it is likely to fail if the direction of ψ completely reverses in (43). This phenomenon seems to occur just near the leeward portion of the separation line ℓ_s and prevents us from fixing its position and properties as well as we can for the windward portion of ℓ_s .

IV. GENERAL PROPERTIES OF THE SOLUTION

The computations were carried out for $\alpha = 3^\circ, 6^\circ, 15^\circ, 30^\circ$ and $t = 1/4$. For $\alpha = 6^\circ$ the second form of the governing equations (2.13) - (2.15) was used with a switch to the first form at $S = 0.523$ ($\hat{\xi} = 0.975$), but for all other values of α the third form was used to initiate the computations. The standard box was used for the integration in the (ξ, η, θ) variables until the crossflow velocity changed sign and generally the characteristic box was used subsequently. A number of studies were made with the zig-zag box at $\alpha = 6^\circ$; it was concluded that this variation is less sensitive to the structural properties of the boundary layer and discarded. For example, in the integrations from the leeward line of symmetry λ , the method broke down at $\xi = 0.44$ as against $\xi = 0.35$ with the characteristic box. On the other hand, integrations from the windward line of symmetry λ_w broke down at $\xi = 0.31$ using either method. Various experiments were made with the step lengths: in the ξ -direction r_i varied from 0.01 to 0.1 (Fig. 2), in the θ -direction k_n varied from $2\frac{1}{2}^\circ$ to 10° (i.e. 0.044 to 0.175) and in the η -direction h_j varied from a minimum of 0.036 near the surface to a maximum of 3.7 at the outer edge when negative crossflow was well developed and the boundary-layer thickness had reached 30. No attempt was made to investigate the effects of h^2 -extrapolation or other deferred approaches to the limit on the results obtained.

The velocity profiles individually show no new general features from those reported by earlier authors (Wang 1974a,b,c, 1975, Geissler 1975) and will not be discussed in detail here. The growth of the boundary layer in the region of crossflow reversal has already been noted, but in contrast to the results obtained by Cebeci et al (1980) for the paraboloid ($t = 0$) we find that the thickness of that part of the boundary layer in which $g < 0$ does not

increase significantly. Thus when $\alpha = 30^\circ$ that part of the boundary layer never extended beyond $\eta = 2$ even though uniform conditions might not be achieved until $\eta = 30$.

The discussion is concentrated on the principal features of the boundary layer, namely the skin friction and the effective blowing velocity which it induces on the external flow. From the equation of continuity (2.1) we know that v asymptotes to a linear function of y as $y \rightarrow \infty$ on the boundary layer scale. Let us define

$$v_\infty(\xi, \theta) = \lim_{y \rightarrow \infty} \left\{ v + \frac{y}{h_1 h_2} \left[\frac{\partial}{\partial x} (h_2 u) + \frac{\partial}{\partial \theta} (h_1 w) \right] \right\}. \quad (4.1)$$

Then the perturbation to the inviscid flow caused by the boundary layer may be regarded as a replacement of the condition of zero normal velocity on the body by the requirement that it be equal to v_∞ . Equivalently, the condition that the body be a streamline surface is changed to the condition that the streamline surface through the forward stagnation point S_0 is at a distance δ^* from the body where

$$\frac{\partial}{\partial x} (h_2 u_e \delta^*) + \frac{\partial}{\partial \theta} (h_1 w_e \delta^*) = h_1 h_2 v_\infty; \quad (4.2)$$

δ^* can be found by solving this equation with the initial condition $\delta^* = 0$ at S_0 . By reference to (3.2) we may connect v with e and hence, after setting $u_\infty = a = v = 1$ and

$$E_\infty = \lim_{\eta \rightarrow \infty} \left[e + \eta \left(\frac{1}{h_1} \frac{\partial f}{\partial \xi} + \frac{1}{h_2} \frac{\partial g}{\partial \theta} + f \left(\frac{1}{2s} - K_2 \right) \right) \right], \quad (4.3)$$

we have

$$v_\infty = E_\infty s^{1/2}. \quad (4.4)$$

The principal quantities on which we shall base our discussion of the solution properties are p_w , q_w and E_∞ , the components of the skin friction in the ξ, θ directions being

$$s^{-\frac{1}{2}}[p(\xi, n, 0), q(\xi, n, 0)] = s^{-\frac{1}{2}}(p_w, q_w). \quad (4.5)$$

The equivalent physical quantities may now easily be deduced on restoring the appropriate values of u_∞ , a , v .

In presenting the results, we shall pay closest attention to the solutions for $\alpha = 6^\circ$ and for $\alpha = 30^\circ$, the first because the ok is well-developed yet a largely complete solution can be found, and the second because the ok has penetrated almost to the nose ($\xi \approx -0.83$) and furthermore the accessibility boundary λ_A differs most clearly from λ_S on the leeside. The next significant stage in the development of λ_A with increasing α occurs at $\alpha \approx 42^\circ$, where λ_S joins up with an incipient nose separation and the whole of the leeside of λ_S becomes inaccessible. Careful studies of the boundary layer have been made in this situation by Wang (1974b) and we see no reason to repeat them.

In Figs. 5, 6 we show the variation of p_w , q_w , E_∞ over the majority of the accessible region lying upstream of λ_S . Perhaps the most interesting result is that $E_\infty < 0$ over a significant part of the region of negative crossflow. Thus the commonly held view that boundary layers under adverse pressure gradients act as injection sources with respect to the external flow is seen not to be universally correct and fails, in particular, near the leeside line of symmetry λ when the pressure gradient is as we have prescribed. It does not necessarily follow of course that $\delta^* < 0$ in this region, but we note that for the paraboloid ($t = 0$) discussed by Cebeci et al (1980) the value of δ^* tends exponentially to $-\infty$ at infinite distances downstream from the nose according to the asymptotic formula derived there. The negative values of E_∞ may be inferred from Wang's studies (1974a, p.38) when it is borne in mind that in his notation

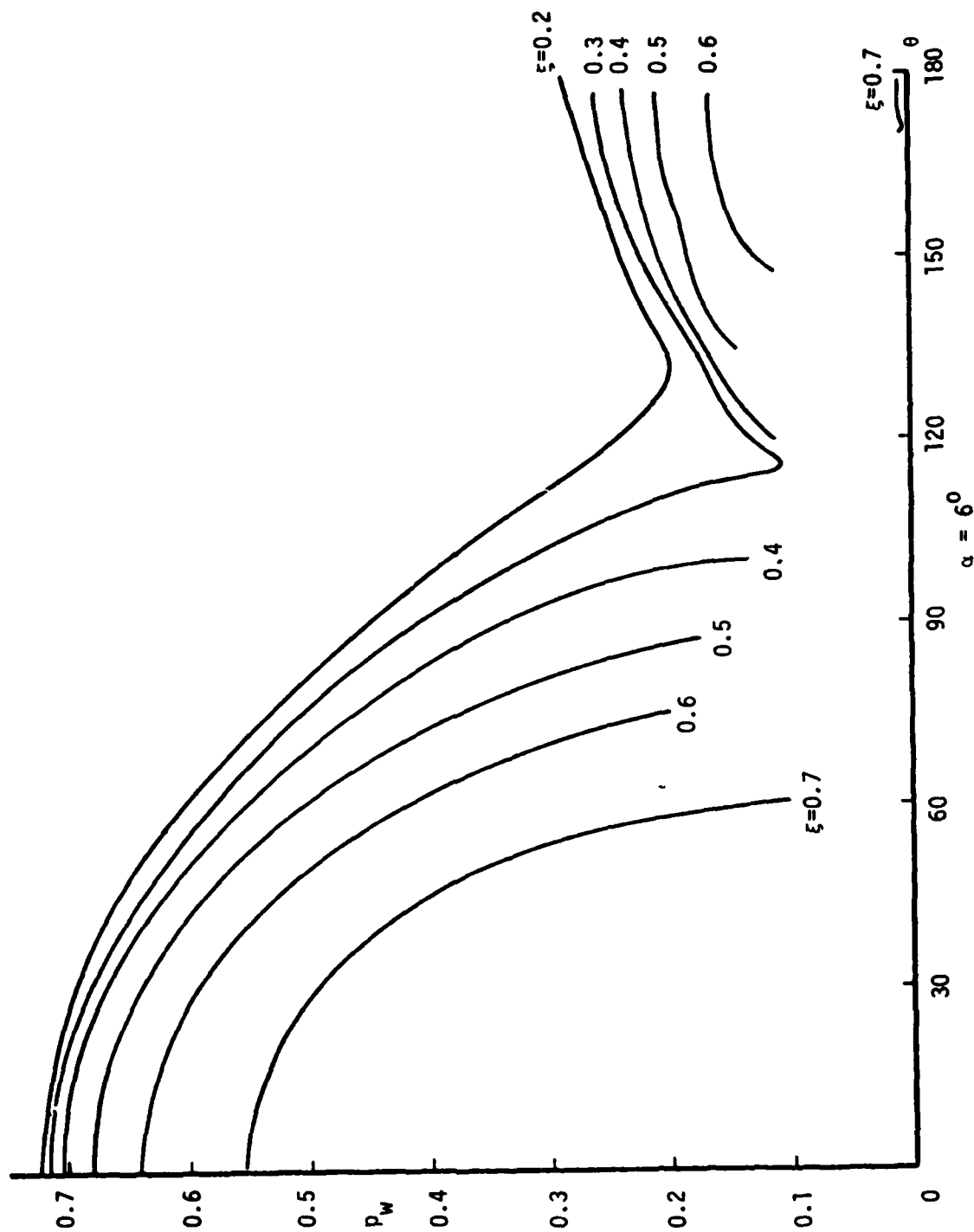


Figure 5a. Variation of the longitudinal component of wall shear parameter p_w around the circumference of the body for different ξ -values, $\alpha = 60^\circ$.

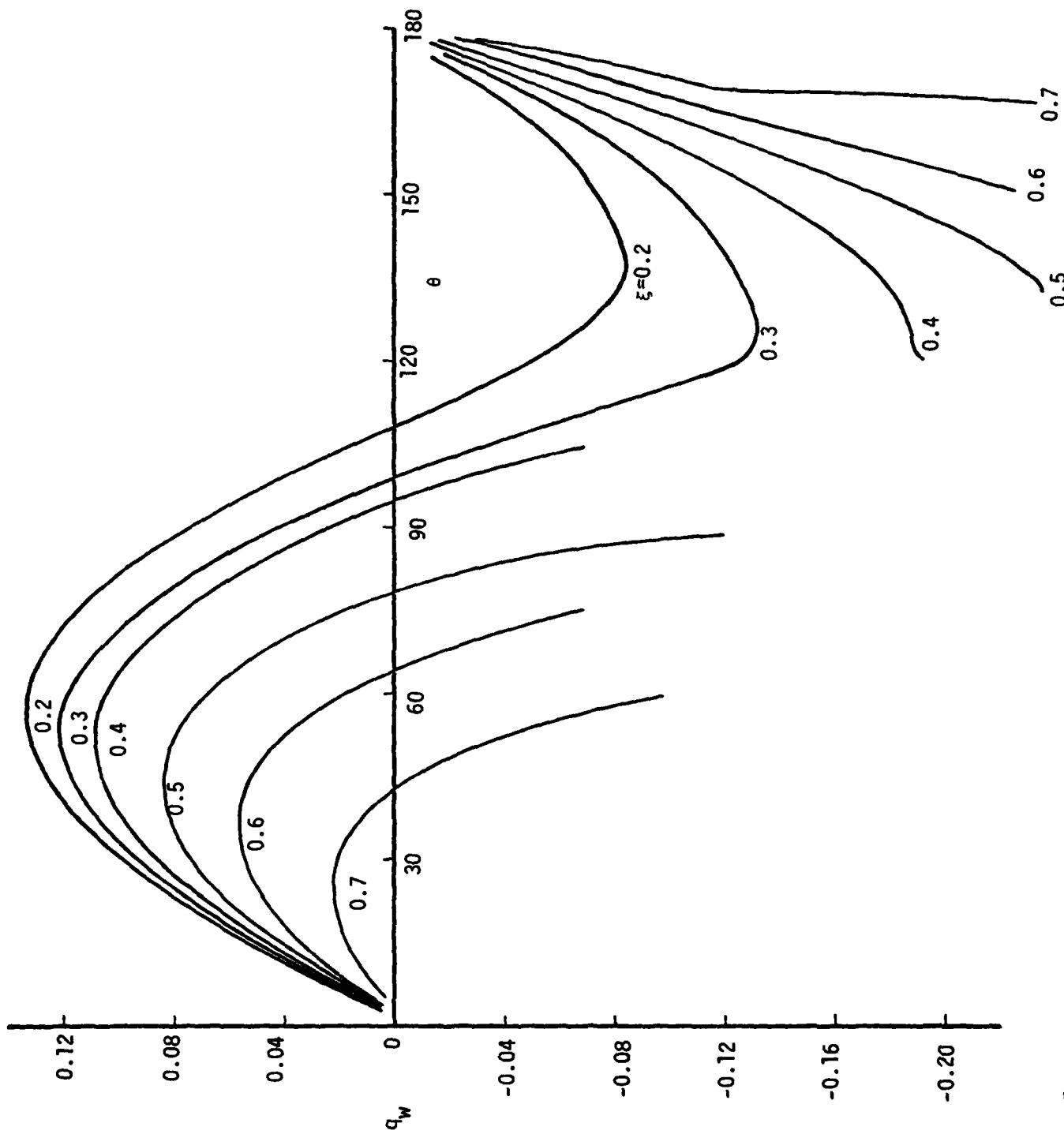


Figure 5b. Variation of the transverse component of wall shear q_w around the circumference of the body for different ξ -values, $\alpha = 60^\circ$.

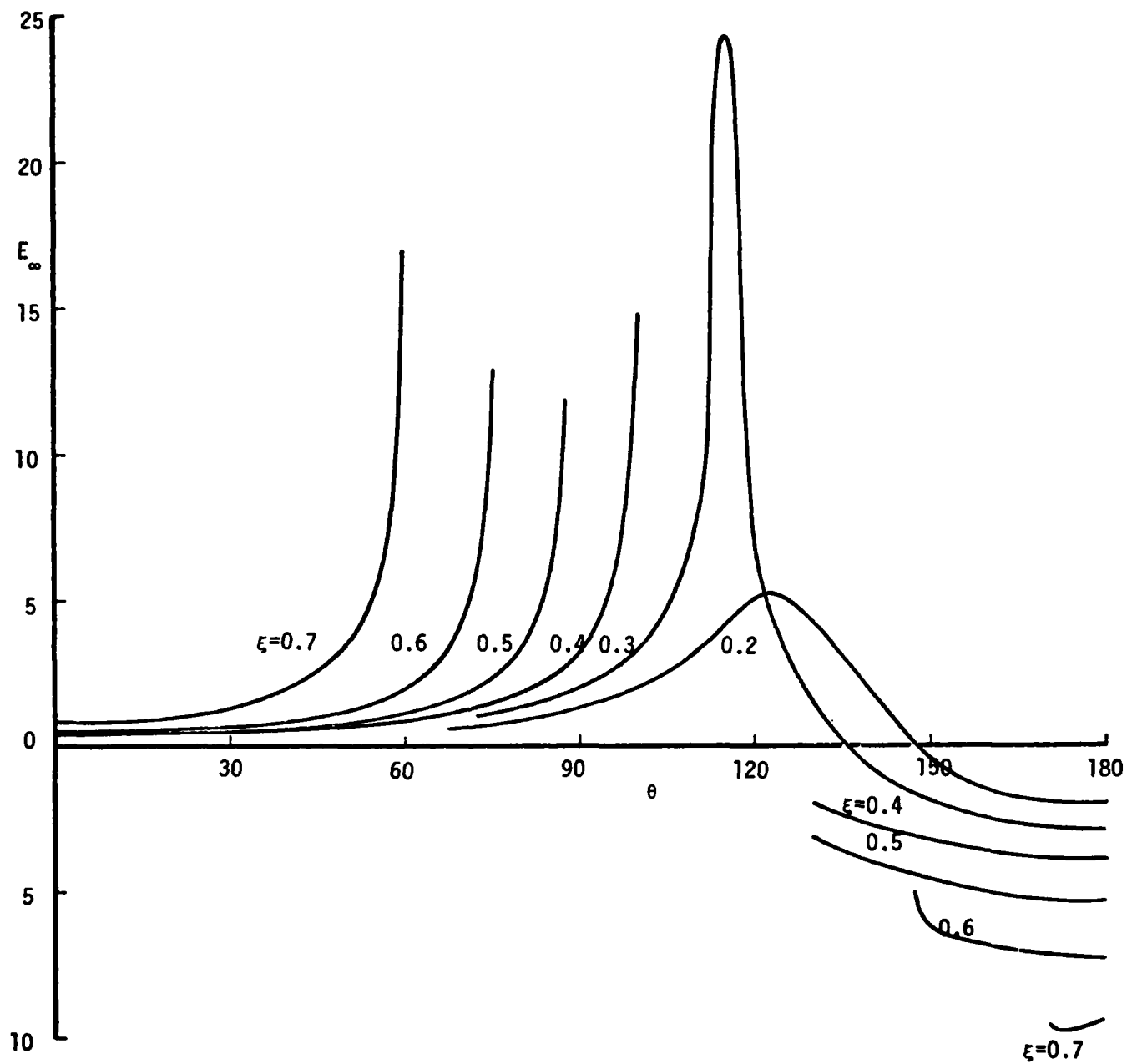


Figure 5c. Variation of the normal velocity parameter E_∞ around the circumference of the body for different ξ -values, $\alpha = 6^\circ$.

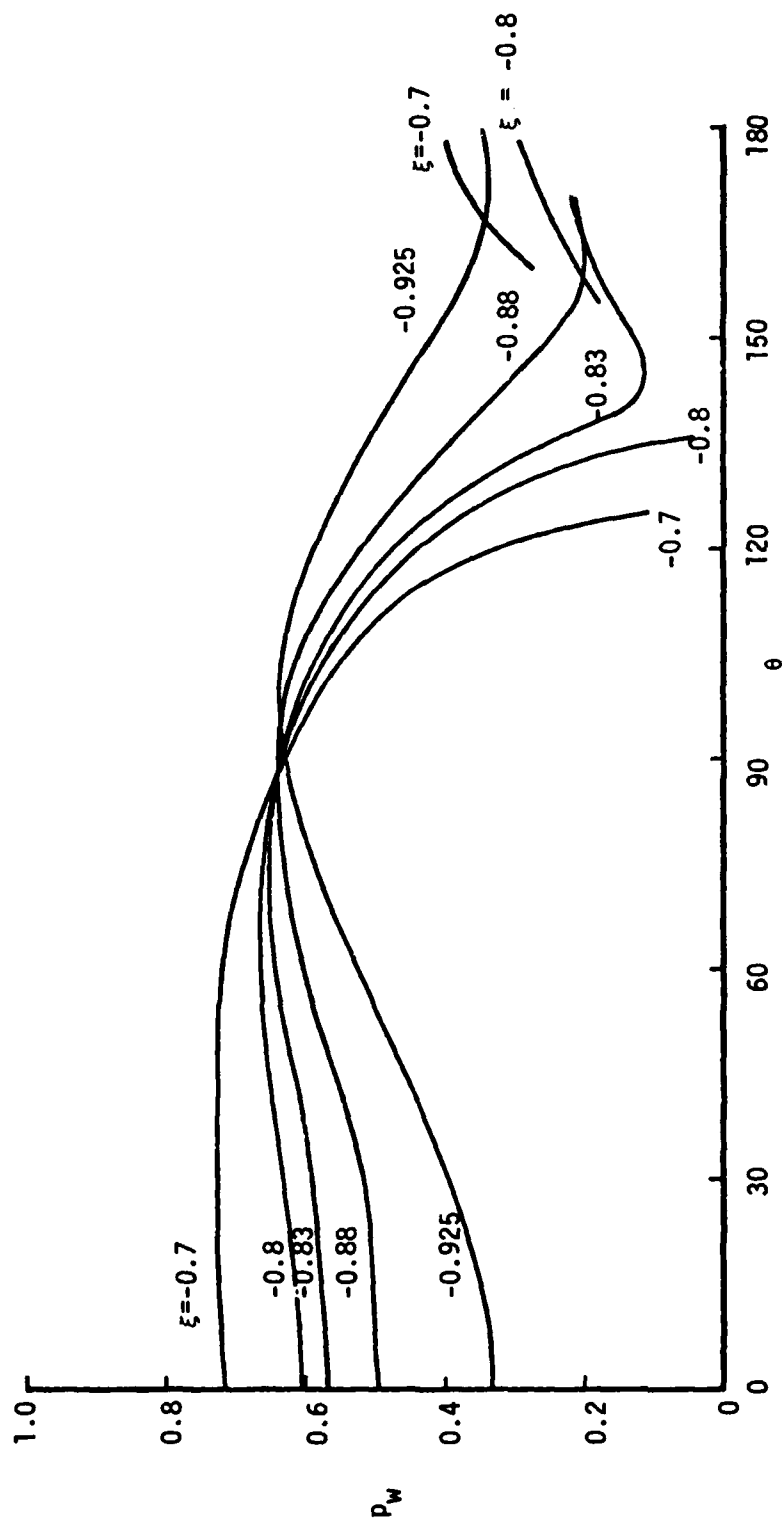


Figure 6a. Variation of the longitudinal component of wall shear parameter p_w around the circumference of the body for different ξ -values, $\alpha = 30^\circ$.

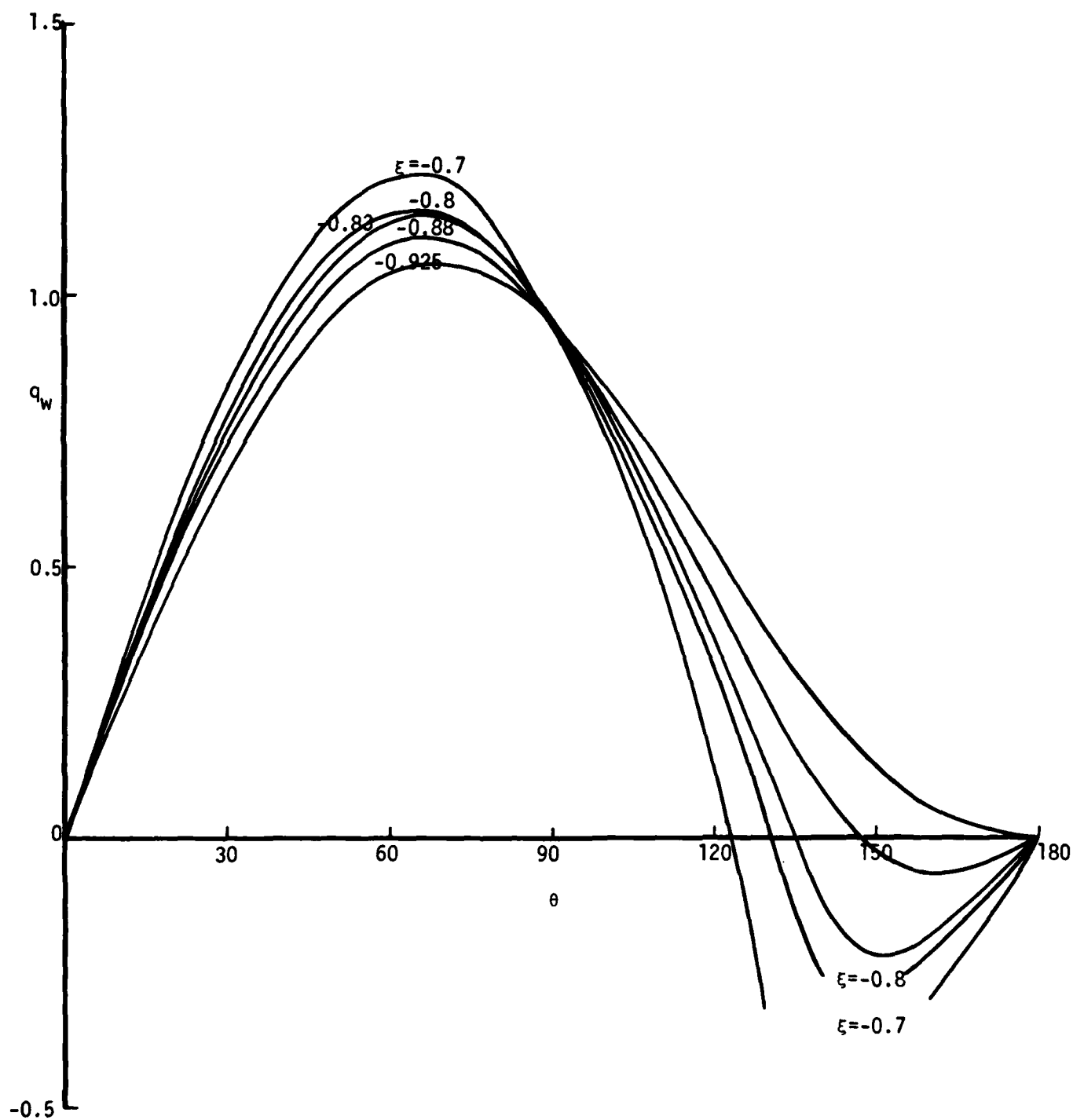


Figure 6b. Variation of the transverse component of wall shear parameter q_w around the circumference of the body for different ξ -values, $\alpha = 30^\circ$.

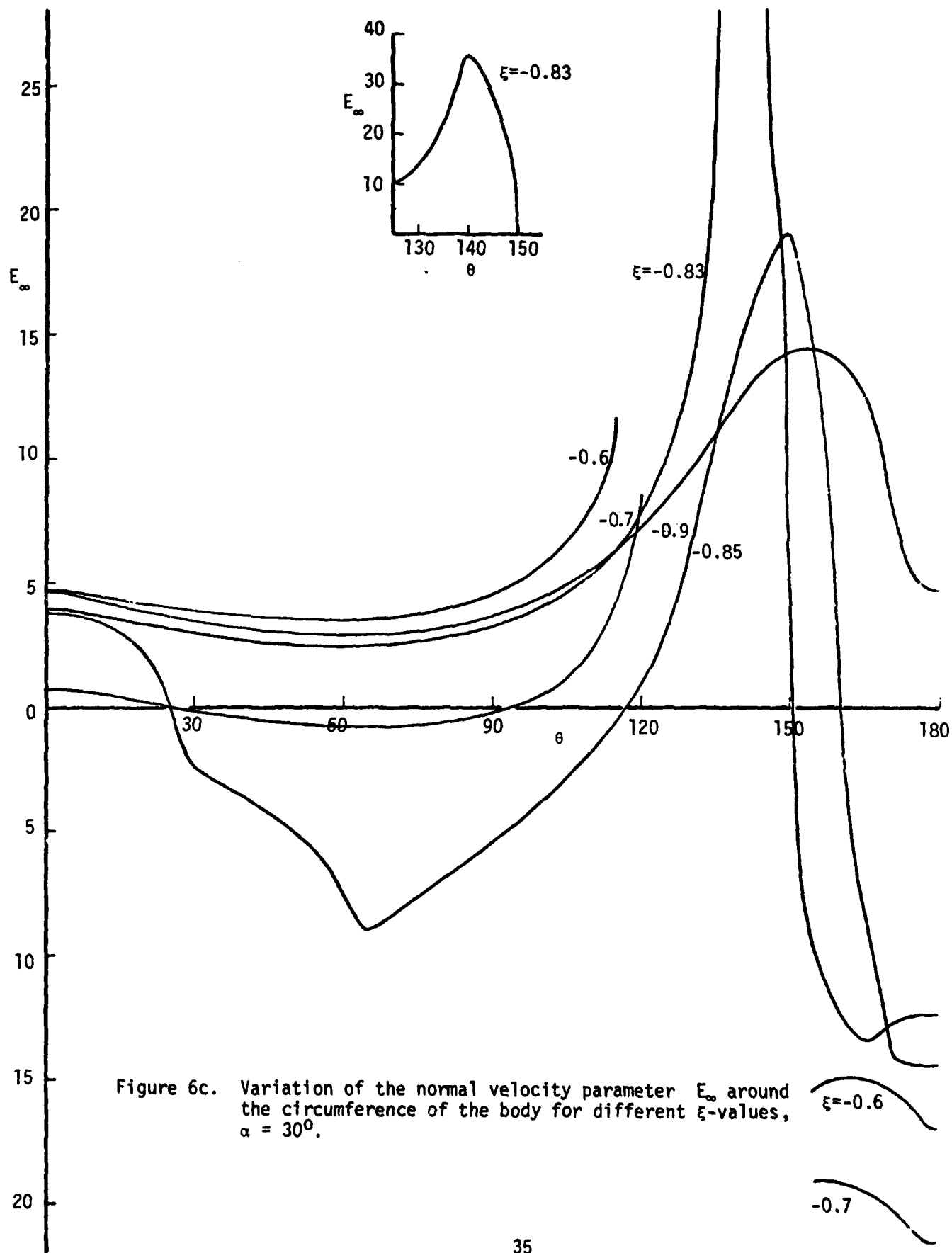


Figure 6c. Variation of the normal velocity parameter E_∞ around the circumference of the body for different ξ -values, $\alpha = 30^\circ$.

$$v_{\infty} = \frac{1}{h_{\theta} h_{\mu}} \frac{\partial}{\partial \mu} (h_{\theta} q \Delta_{\mu}^*) + \frac{1}{h_{\theta}} \frac{\partial}{\partial \theta} (h_{\mu} q \Delta_0^*). \quad (4.6)$$

The principal interest in the plots of the skin-friction lines is in the location of ℓ_s and its nature. The location of the line of zero crossflow skin friction is shown in Fig. 7 for the various values of α . Good agreement is obtained with the specific results of Geissler (1975) at $\alpha = 15^\circ$ and of Patel and Choi (1979) at $\alpha = 6^\circ$, but there are significant differences with Wang's data (e.g. 1975).

In Fig. 7 we also plot our best estimates of the separation lines ℓ_s for the same values of α . The principal properties of the solution near ℓ_s are discussed in detail in the next two sections but broadly on the windward side its shape is deduced by a combination of numerical analytic arguments but on the leeside it is essentially determined by the failure of the numerical scheme as θ decreases. In addition we have superposed on these diagrams the external streamlines and we see that at $\alpha = 15^\circ, 30^\circ$ and on the leeside of ℓ_s they are pointing into the region of computation. In accordance with Raetz's notion of zones of influence, it follows that the solution in part of this region cannot be completed with the information supplied in this report. For information is also necessary from the separated region downstream of ℓ_s which we are unable to compute. Thus the definition of separation as the limit of the accessible region from the nose is apparently not compatible either with it being a limiting streamline or an envelope of streamlines. We shall return to this point below.

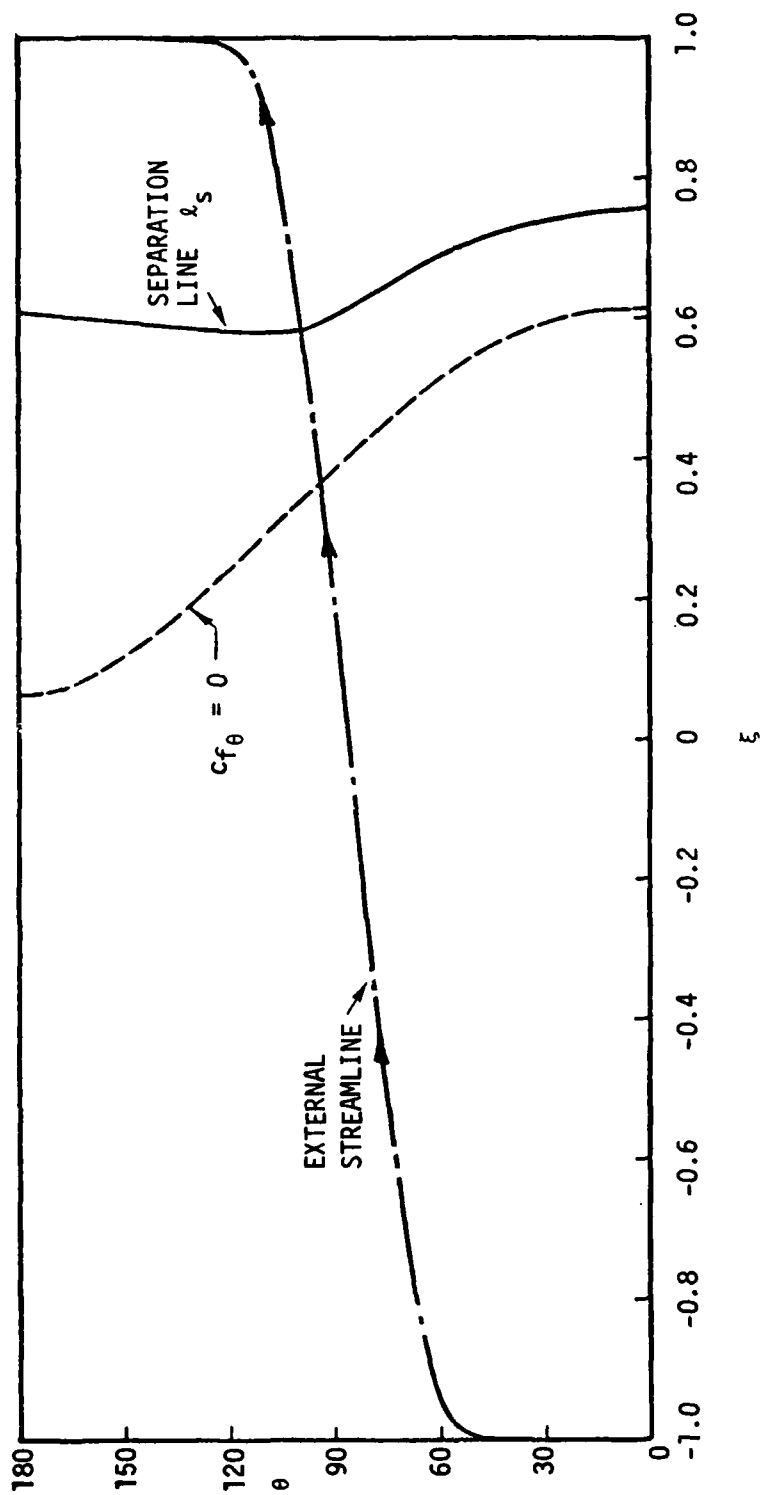


Figure 7. External streamlines, zero- cf_θ lines and separation lines. (a) $\alpha = 3^\circ$.

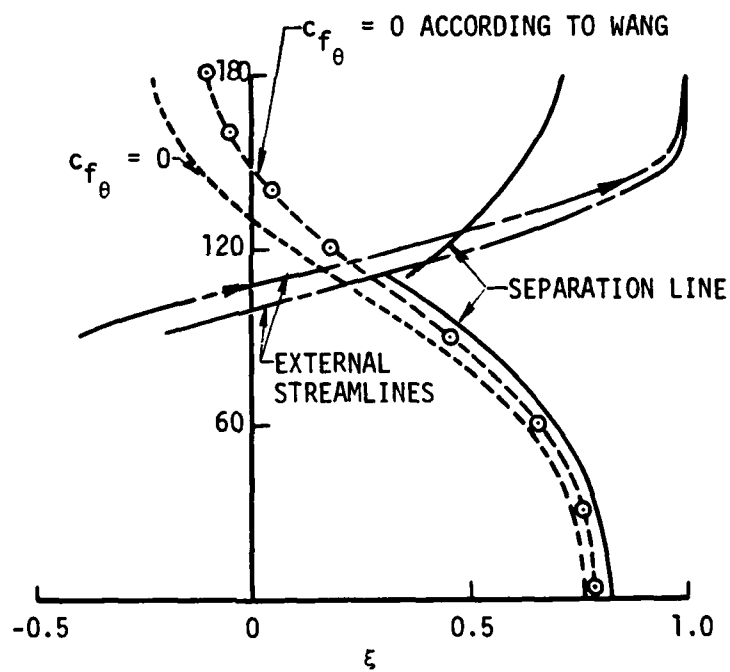


Figure 7. (b) $\alpha = 6^\circ$.

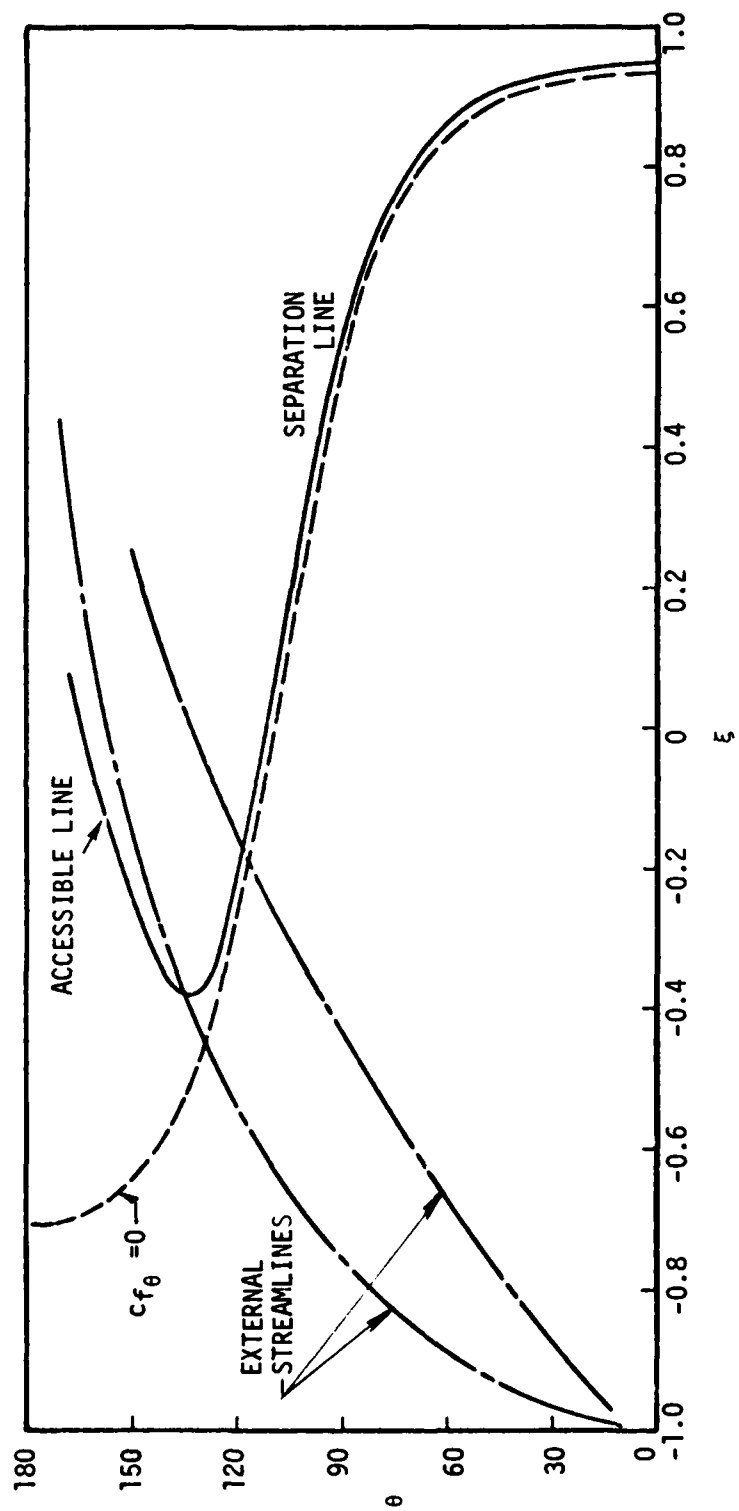


Figure 7. (c) $\alpha = 15^\circ$.

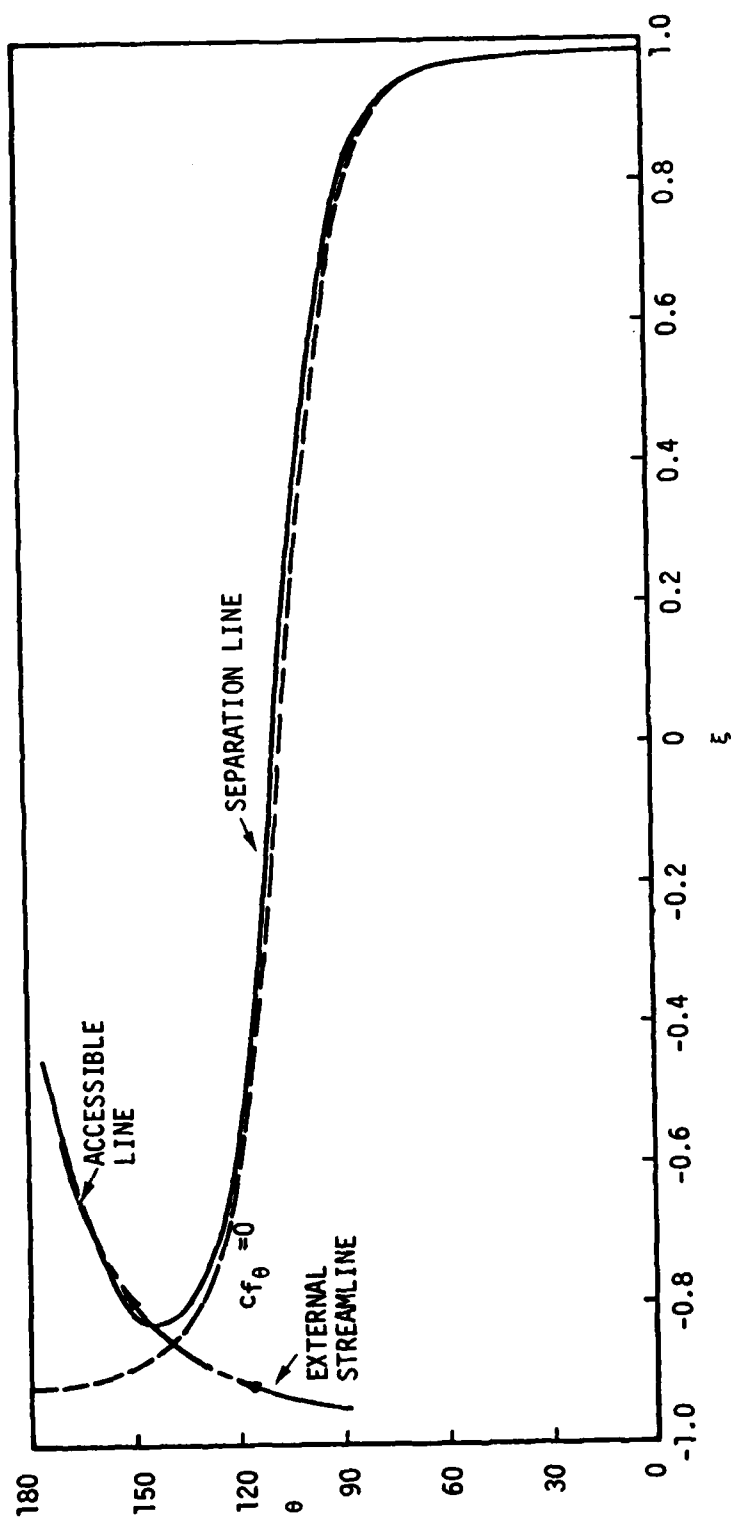


Figure 7. (d) $\alpha = 30^\circ$.

4.1 The Separation Line When $\alpha = 6^\circ$

An important goal of our numerical studies is to clarify further the nature of the separation line ℓ_s . For this reason particular attention was paid to the properties of the solution in its neighborhood when $\alpha = 6^\circ$. The conclusions we are able to come to for this special angle of incidence may then be used to comment on the nature of ℓ_s for other values of α . There is no doubt that when ℓ_s intersects either the windward line of symmetry ℓ_w (at $\xi = 0.84$) or the leeward line of symmetry ℓ (at $\xi = 0.72$), the solution develops a singularity of the Goldstein type (Goldstein 1948, Brown 1965). We may also expect (Buckmaster 1971) that at these points ℓ_s is perpendicular to ℓ_w, ℓ and further that in their neighborhoods it coincides with the accessibility boundary ℓ_A .

There are several conflicting views about the flow properties at general points of ℓ_s . Let us suppose first of all that ℓ_s is a continuous curve joining $(\xi, \theta) = (0.84, 0)$ to $(0.72, \pi)$ but is not necessarily monotonic. Thus we postpone discussion of Wang's (1976a) concept of open separation until later. In this case there has been general support for Hayes (1951) concept of ℓ_s , or strictly, the normals to the surface through ℓ_s , as a bound of those points for which the boundary layer can be computed starting from the forward stagnation point and making use only of conditions at $\eta = 0$ and as $\eta \rightarrow \infty$. Beyond this bound the solution depends in some way on conditions further downstream and in particular at the rear stagnation point. We concur with the notion that our forward integration procedure cannot continue the solution beyond ℓ_s but we have strong reservations about the implication that it may be continued as far as ℓ_s in all cases. When $\alpha \leq 6^\circ$, however, the identification of ℓ_A and ℓ_s is in our view largely complete.

The main controversy about ℓ_s in the literature centers on whether it is an envelope of limiting streamlines, i.e. skin-friction lines, (Eichelbrenner

and Oudart 1954, 1973, Maskell 1955) or is itself a limiting streamline (Lighthill 1963). The distinction is not academic. In fact it is of crucial importance in the study of practical boundary layers, whether laminar or turbulent, because if the first view is correct then, unless special preventative measures are taken, a singularity must develop in the solution at all points of ξ_s . In this event the slope of the displacement surface also becomes infinite at ξ_s and the boundary layer exerts a serious modifying influence on the mainstream. Thus the hierarchical method of studying high Reynolds number flows fails, just as it does in two dimensions. Experimentally inspired statements about ξ_s are therefore not germane to the question, for in a practical flow the solution must be regular and Lighthill's notion of it being a limiting streamline is correct. However, it is at present virtually impossible to prescribe the correct pressure gradient and, if it turns out that a general pressure gradient leads to a singularity, there are important consequences. For example, a general interaction theory of the kind investigated by Smith (1977, 1978) will almost certainly be necessary to treat the solution in the neighborhood of ξ_s .

We can see how the singularity must develop at ξ_s if it is an envelope of limiting streamlines as follows. Suppose that ξ_s is given by $\xi = \xi_s$ for all θ and near $\xi = \xi_s$ the two components of skin friction are

$$\tau_\xi = (\xi_s - \xi)^\beta \quad \tau_\theta = 1 \quad \beta > 0 \quad (4.7)$$

Then the limiting streamlines are the curves

$$\theta = \theta_1 - \frac{1}{1-\beta} (\xi_s - \xi)^{1-\beta} \quad (4.8)$$

where θ_1 is a parametric constant. Thus if $\beta < 1$ these curves touch ξ_s at $\theta = \theta_1$, whereas if $\beta = 1$ (corresponding to a regular solution) they meet it at $\theta = \infty$.

After careful examination of the numerical data near the termination of our calculations, we obtained strong but not totally convincing evidence that

the separation line is an envelope and we are led to make the hypothesis that this property holds over the whole of its accessible length. The notion is, however, not without its difficulties, especially on the leeward side.

Let us begin by looking at the calculations in the neighborhood of x_s on the windward side, i.e. for $\theta < 110^\circ$ (Fig.7b). As explained in Section III, when we integrate the equations at a given value of ξ for increasing values of θ starting from x_w , where $\theta = 0$, our procedure is to use the standard box until the crossflow velocity $w(=g)$ changes sign. Then we switch either to the zig-zag box or, more usually, to the characteristic box, both of which take into account to an increasing degree the fact that information is being fed to the new (ξ, θ) station from larger as well as smaller values of θ . As θ increases further, a stage is reached when neither of these boxes can be used through lack of information from the next θ station at the previous ξ station (the points $(i-1, j, m+1)$ in Fig. 3b) or because p becomes negative or because the iterations fail to converge. In the first eventuality the standard box is used for one further θ station and the calculations at this ξ station are terminated. This procedure is rather crude and it is desirable for a full understanding of the separation singularity that a superior way of overcoming the difficulty be found.

A new set of values of p_w, q_w, E_∞ is displayed in Table 1; they correspond to a representative value 0.7 of ξ and at values of θ near the termination of the calculations which occurred at $\theta = \pi/3 (=60^\circ)$. At this station due to the lack of any information about the solution at $\xi = 0.69$ and $\theta = 62.5^\circ$; the wall shear parameter p_w became negative after only two iterations causing the iterations to diverge. For this data we infer that the separation line passes close by $(0.7, \pi/3)$ and that the solution is not smooth there.

Table 1. Computed values of p_w, q_w, E_∞ at $\xi = 0.7, \alpha = 6^\circ$. The θ step length in radians is $\Delta\theta = 0.0437$ and the values of E_∞ were actually calculated at midway stations in both ξ and θ .

θ°	p_w	q_w	E_∞	$(p_w + \frac{1}{3} q_w)^2$	$\frac{1}{3} p_w - q_w$	E_∞^{-2}
42.5 $^\circ$	0.413	+0.002	2.091	0.172	0.136	0.229
45 $^\circ$	0.394	-0.005	2.412	0.154	0.136	0.172
47.5 $^\circ$	0.369	-0.014	2.857	0.136	0.137	0.123
50 $^\circ$	0.343	-0.024	3.468	0.118	0.139	0.083
52.5 $^\circ$	0.313	-0.035	4.254	0.091	0.139	0.055
55 $^\circ$	0.279	-0.049	5.415	0.069	0.140	0.034
57.5 $^\circ$	0.233	-0.066	7.692	0.045	0.144	0.016
60 $^\circ$	0.104	-0.098	16.94	0.005	0.133	0.003

We now test the hypothesis that the separation line is an envelope of limiting streamlines. On this assumption, Brown (1965) has studied the nature of the solution near separation and her conclusions may be interpreted in the present context as follows: Let (ξ_s, θ_s) be a point P_s on the separation line λ_s , which makes an angle θ_s with the ξ -direction. At P_s the component τ_s of the skin-friction along the direction of λ_s is finite while the normal component τ_n vanishes. Her theory predicts that at a point Q on the normal to λ_s through P_s

$$\tau_s = A_s + B_s (QP_s)^{\frac{1}{2}} + \dots \quad \text{when } QP_s \ll 1 \quad (4.9a)$$

while

$$\tau_n = C_s (QP_s)^{\frac{1}{2}} + \dots \quad \text{when } QP_s \ll 1 \quad (4.9b)$$

where A_s, B_s, C_s are numbers with $C_s > 0$. We now tabulate $p_w - \tan\theta q_w$ and $p_w \tan\theta - q_w$ as functions of θ for various θ . These functions are not quite the τ_n, τ_s of (4.9) since the θ -direction is not normal to ℓ_s but these differences are not thought to be significant and the final value of θ chosen must be consistent with the predictions of the separation point at $\xi = 0.70$ and at neighboring values of ξ . We conclude that the best value of $\tan\theta = -1/3$, corresponding to $\theta_s \approx -19^\circ$ and display in Table 1 the values of $(p_w + 1/3 q_w)^2$ and of $1/3 p_w - q_w$. It is seen that $(p_w + 1/3 q_w)^2$ is roughly linear, in agreement with (1), except very near $\theta = 60^\circ$ and we infer that separation occurs at $\theta_s = 60.5^\circ$. A more cautious conclusion is that $(p_w + 1/3 q_w) \sim (\theta_s - \theta)^n$ where $1/3 \leq n \leq 1/2$ as $\theta \rightarrow \theta_s^-$, but in view of the complexity of the numerical program, the slight irregularity visible in the data of Table 1 and the difficulty in reproducing singularities by numerical integration, we are broadly satisfied that these results are consistent with Brown's theory. The function $p_w - 1/3 q_w$ is almost constant except right near $\theta = 60^\circ$, where the second term in (4.9a) might be important but it is more likely that the program is inadequate to predict this term. Finally we display E_∞^{-2} , which should be linear in θ with a zero at $\theta = \theta_s$. This is reasonably the case except near $\theta = \theta_s$, but the predicted value of θ_s from this set of values in Table 1 is approximately 59° , rather less than that predicted from p_w, q_w , especially when it is borne in mind that E_∞ is tabulated for $\xi = 0.695$.

After repeating these arguments at all the ξ -stations on the windward side we are able to determine ℓ_s from $\xi = 0.31$, where $\theta_s = 113^\circ$, to $\xi = 0.83$, where $\theta_s = 0$, and confirm that its shape is consistent with the choice of θ in tables similar to Table 1. We conclude that on the windward side ℓ_s is indeed an envelope of limiting streamlines and that the skin friction τ_s on it ($= p_w \sin\theta - q_w \cos\theta$) varies from ≈ 0.13 at $\xi = 0.31$ to a maximum

≈ 0.15 at $\xi = 0.6$, decreasing afterwards to zero when ℓ_s intersects the windward line of symmetry. The shape of the separation line is shown in Fig. 7b and the variation of τ_s along it in Fig. 8. Along ℓ_w , ℓ_s is perpendicular to ℓ_w in agreement with Buckmaster's (1971) theory of the structure of the separation line in this neighborhood.

On the leeward side the situation is much more difficult to interpret with confidence. First of all, in the integration from $\theta = \pi$ no separation is observed for $\xi < 0.35$, even though from the windward side it occurs at $\xi = 0.31$ and when $0.31 < \xi < 0.35$ the two integrations give results closely in agreement for $\theta < 100^\circ$. If separation does occur, it is very weak and may have been missed in the numerical calculation from ℓ because, even with the use of the characteristic box there is a slight loss of precision in integrating against the cross-stream direction outside the boundary layer, especially as $g > 0$ for all θ when $n > 3$ and $\xi \leq 0.35$. The first onset of separation, at $\xi = 0.35$, occurs when $\theta < 110^\circ$ which is less than the value of θ_s at $\xi = 0.31$ according to the calculation from the windward side. We believe that the discrepancy between the windward and leeward integrations is largely the fault of the latter and that, bearing in mind the very sharp peak in E_∞ at $\xi = 0.30$ (see Fig. 5c), separation occurs first close to $(0.31, 113^\circ)$.

For $\xi \geq 0.35$ the integration from $\theta = \pi$ breaks down at values of $\theta \geq 110^\circ$ in a curious way. As θ decreases p_w decreases slowly, q_w increases steadily and E_∞ remains almost constant. As the calculations draw to an end p_w begins to fall more rapidly towards negative values, sometimes sharply, and the integration then terminates either by a failure to converge or a lack of information from the previous

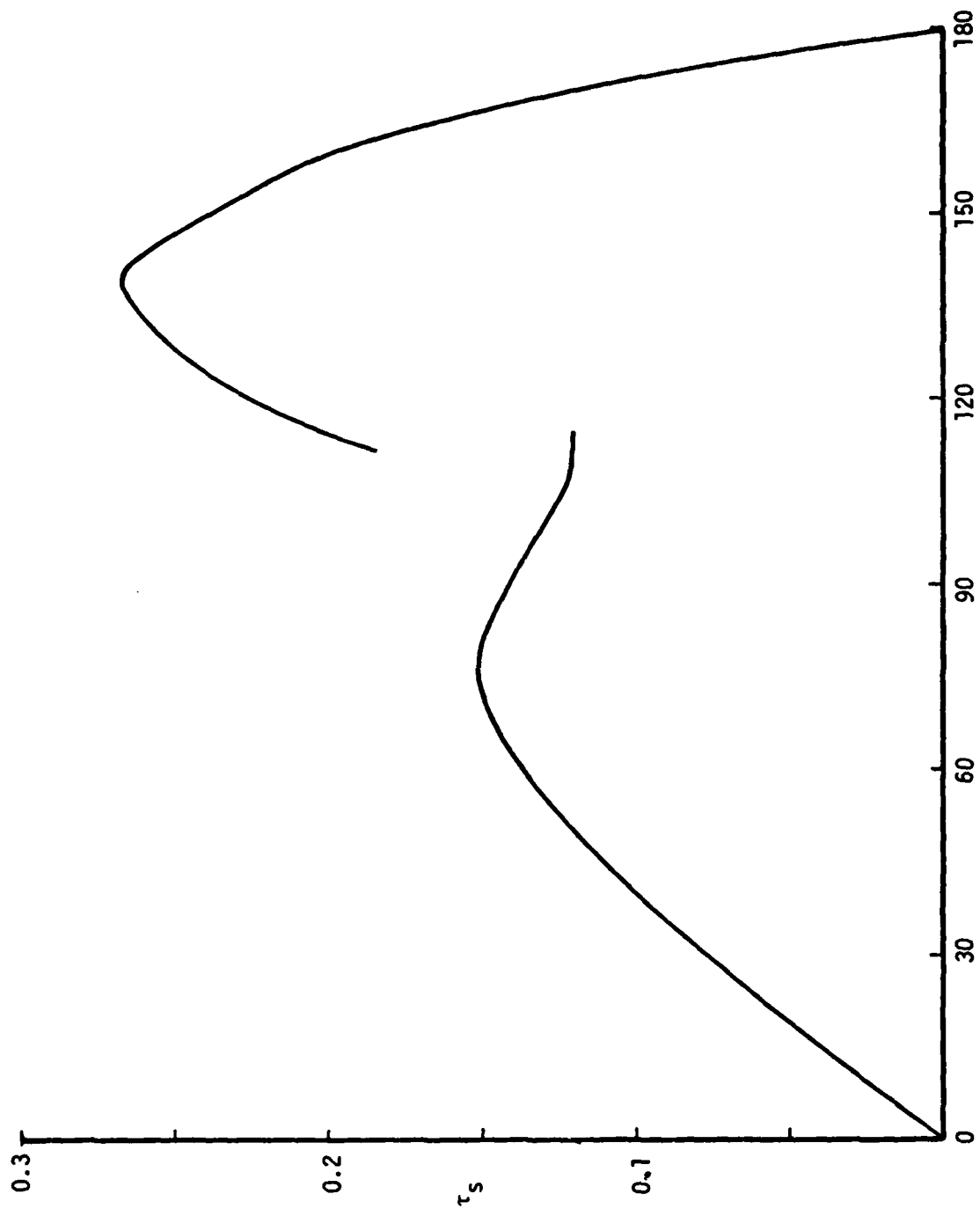


Figure 8. The variation of tangential component of reduced skin friction ($=p_w \cos \theta_s - q_w \sin \theta_s$) on θ_s for $\alpha = 6^\circ$.

ξ station, even within the requirements of the standard box. These causes of failure occurred roughly in the ratio 2:3, respectively. We give a set of results in Table 2 for $\xi = 0.6$ typical of the situation where termination occurs through lack of the necessary data. The sudden onset of breakdown makes unprofitable a study of the solution properties near λ_s of a similar kind to that just carried out for the windward side. It is clear that something odd is happening, but Brown's theory is of little direct help.

Table 2. Computed values of p_w , q_w , E_∞ at $\xi = 0.6$, $\alpha = 6^\circ$. The step length in radians is $w_{k_n} = 0.0437$ and the values of E_∞ are actually calculated at midway stations in both ξ and θ .

θ	p_w	q_w	E_∞
165	0.156	-0.120	-6.94
162.5	0.154	-0.139	-6.84
160	0.151	-0.158	-6.76
157.5	0.148	-0.176	-6.67
155	0.146	-0.193	-6.52
159.5	0.144	-0.210	-6.36
150	0.121	-0.226	-6.08
147.5	0.120	-0.215	-4.99

Let us suppose that λ_s is here also an envelope of limiting streamlines — the alternative, that it is itself a limiting streamline seems excluded by the breakdown of the iterative process at the final value of θ . Then either the limiting streamlines turn upwards before touching λ_s , as in Fig. 9a, or turn back, as in Fig. 9b). The first alternative seems unlikely



Figure 9. Two optional limiting streamline patterns near leeward part of ℓ_s .

from the available data since q_w shows no signs of becoming positive. The second requires p_w to change sign, which is more consistent with the data as the final computed value of p_w is often less than half its value near $\theta = \pi$. It also agrees with the Buckmaster theory, which applies when ℓ_s intersects ℓ .

If the Brown structure holds very near to ℓ_s , the skin friction τ_s along ℓ_s is closely given by the last reasonable values of p_w , q_w and the slope of ℓ_s may be inferred from the line of breakdown of solutions. We can also estimate the variation of τ_s over the range $0.35 < \xi < 0.71$ on the leeward side; it is displayed in Fig. 8. The position of ℓ_s may be inferred as well within an accuracy of about 1° . A necessary requirement for obtaining the solution right up to ℓ_s is that the local streamlines on the normals to the surface through ℓ_s are all directed out of the origin of integration. The most likely streamlines to violate this requirement are those external to the boundary layer, but for $\alpha = 6^\circ$ our estimate for ℓ_s does not lead to a contradiction due to this cause except near the ok. The external streamlines are also indicated in Fig. 7b and are pointing out of the computed region at the

estimated position of ℓ_s . We infer that for $\alpha = 6^\circ$ the boundary of the region accessible from the forward stagnation point is largely defined by the position of ℓ_s .

For the shape of ℓ_s near the ok at $\xi = 0.31$ three possibilities were considered and are shown in Fig. 10. Our preference is Fig. 10a and if we are right, the complicated structures of the limiting streamlines near the ok makes their computation very difficult. Some comments are in order about (b) and (c). The option (b) is inspired by the notion of "open separation" which Wang (1974b) introduced in his study of the solution when $\alpha = 30^\circ$ and, if it occurs, it implies that τ_s vanishes at some point

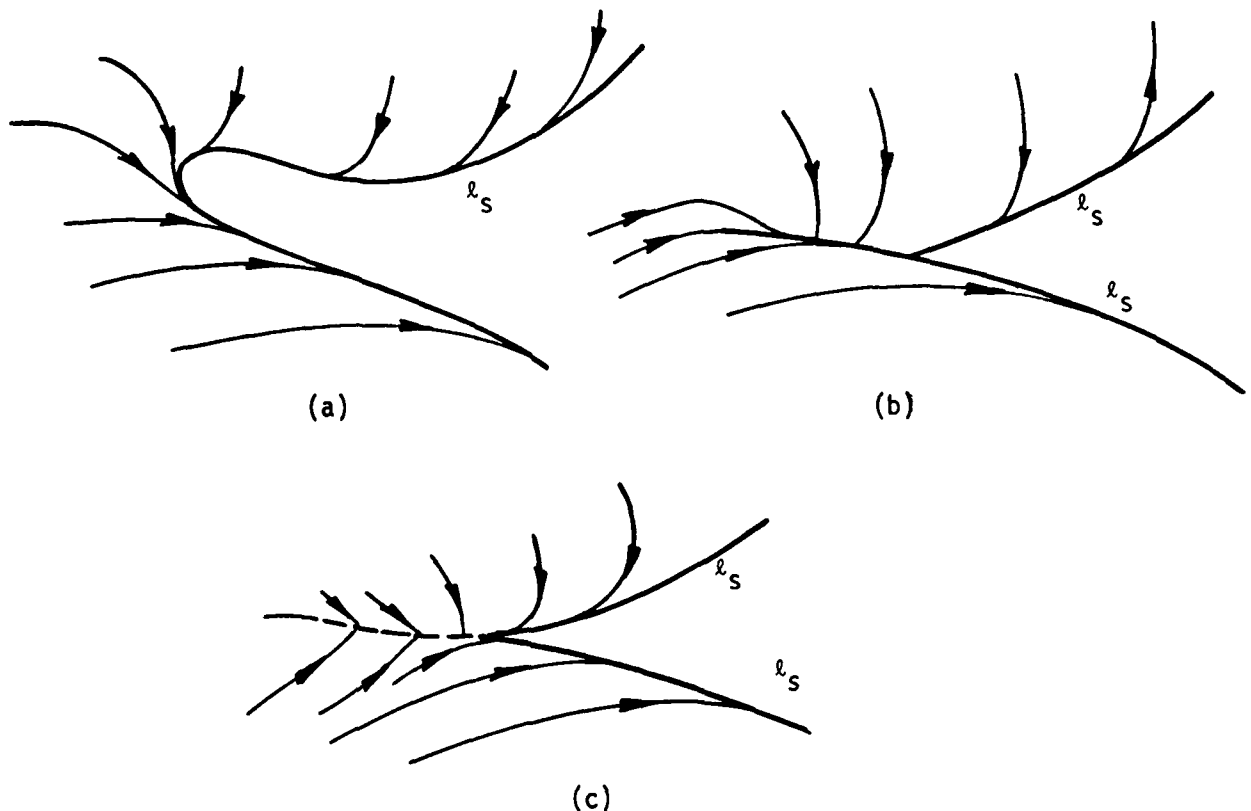


Figure 10. Three optional limiting streamline patterns near the Ok.

of ℓ_s . The option (c) is a weak boundary layer collision (shown by the dotted line) and would be identified in our calculations by a separation line overlap when computed from ℓ and ℓ_w for fixed ξ . It has been found in boundary layer studies on rotating spheres (Banks 1976) and also in the entrance region of a curved duct (Stewartson, Cebeci, and Chang, 1980), where it is preceded by a singularity in the displacement thickness. Our calculations (Fig.5c) indicate that a singularity in E_∞ is very close to $(0.30, 113^\circ)$, but they are not as smooth in this neighborhood as we should like and a clarification of the structure might well follow from a refinement in our numerical work.

4.2 The Separation Lines for $\alpha = 3^\circ, 15^\circ, 30^\circ$

When $\alpha = 3^\circ$ the first signs of irregularity are the rapidly increasing values of E_∞ for $\theta \approx 105^\circ$ as ξ approaches 0.545. The windward integration breaks down at $(0.545, 110^\circ)$ with p_w rapidly approaching zero as this point is reached. The leeside computation may be continued to $\theta = 0^\circ$ at $\xi = 0.545$ but the maximum value of E_∞ is 11 at $\theta = 100^\circ$ suggesting that separation is near. At $\xi = 0.60$ the leeside computation breaks down at $\theta = 120^\circ$ and at $\xi = 0.625$ no solution can be obtained since separation has already occurred at $\theta = 180^\circ$. The windward calculations behave similarly to those for $\alpha = 6^\circ$. We infer that ℓ_s is closed, and the normals through it very largely, if not entirely, define the accessibility limit ℓ_A . It is noted that the general shape of ℓ_s was forecast by Wang (1976).

When $\alpha = 15^\circ$ the first sign of difficulty in the numerical computation occurs at $\xi = -0.475$ when an irregularity develops in the windward integration at $\theta = 135^\circ$; in addition $E_\infty(\xi, 135)$ reaches a value of 14 at this point, which suggests that separation is near. Breakdown first occurs

at $(-0.425, 135^\circ)$ as the calculations advance from the windward side. At $\xi = -0.400$ the integrations in both directions break down, at 130° and 135° , the leeside one because the iterations exceed the maximum allowed. For $-0.4 < \xi < 0.1$ the leeside computations come to an end at $\theta = 140^\circ$, and at $\xi = -0.1$ the solution at $\theta = 140$ becomes unacceptable because $|q| > 0.1$ at the outer edge of the boundary layer in a dramatic fashion, no such phenomenon being observed at $\theta = 145^\circ$. Thereafter the lower limit of θ slowly increases with ξ reaching 165° at $\xi = 0.2$. The physical explanation is that the integration at the lower limit of θ should make use of information from even smaller values of θ in the outer part of the boundary layer and cannot do so because this information has to come from the separated part. From Fig. 7c the true lower limit of θ defining the accessible region is almost certainly given by the external streamline from the ok, and the position of ℓ_s on the leeward side is irrelevant to the computations. The computations were arbitrarily terminated at $\xi = 0.200$; although the boundary layer is thick (~ 18) there is no new fundamental reason why they cannot be continued.

On the windward side there are no new features of the solution that need special comment; it is interesting that ℓ_s nearly coincides with the line of zero q_w . The ok region of ℓ_s is difficult to be definite about, there being again the three possibilities of Fig. 10 to consider. In this case also our inclination is to favor Fig. 10a, that ℓ_s is closed in this neighborhood but the evidence is very weak. Wang (1976) favors open separation at $\alpha = 30^\circ$ over a substantial proportion if not all of the leeward part of ℓ_s . In our view the notion of inaccessibility preempts a definite decision on this question.

When $\alpha = 30^\circ$, the first sign of difficulty occurs at $(-0.85, 155^\circ)$ when E_∞ reaches a peak of ≈ 19 suggesting that separation is near. From the windward side breakdown first occurs at $\xi = -0.83$ and $\theta = 140^\circ$ where $p_w < 0$. On the leeward side breakdown also occurs at $\xi = -0.83$ but at $\theta = 146^\circ$; these points are sufficiently close together that their actual coincidence may reasonably be inferred. Continuing with the leeward solution, the ok shows some indication of being similar to that for $\alpha = 6^\circ$ and then the breakdown value of θ slowly increases with θ reaching 156° at $\xi = -0.74$ at which point $|q| > 0.1$ at the outer edge of the boundary layer. As for $\alpha = 15^\circ$, the reason is that the boundary of the accessible region from stagnation is probably upstream of ξ_s . We note that the breakdown in the solution for $-0.83 < \xi < -0.74$ on the leeward side cannot be directly associated with ξ_s and also happens to occur at points practically coincident with the external streamline through the ok . The shapes of this external streamline of ξ_s on the windward side, and of the breakdown curve on the leeward side are displayed in Fig. 7d to demonstrate this property. On the windward side the behavior of ξ_s is similar to that for other values of α and we shall not comment on it.

V. DISCUSSION

The generalization of the Keller box method of solving parabolic differential equations, to take account of the varying direction of the local streamlines from that of the limiting streamline at the body to the external streamline including any overshoots, by the concept of the characteristic box has enabled us to continue accurate solutions of the boundary layer equations further than has been possible hitherto. In fact we believe that the method can be used virtually up to λ_A the boundary of the accessible region from 0.

At zero incidence λ_A and λ_S are coincident circles defined by $\xi \approx 0.79$ (Wang 1970). At $\alpha = 3^\circ$ the two are still coincident but are no longer circles (Fig. 7a) being moved forward on the leeside to $\xi \approx 0.60$ (i.e. for $\theta > 100^\circ$) and curving back to $\xi \approx 0.76$ at $\theta = 0$. A large region of weak reversed circumferential flow develops extending almost to $\xi = 0$ near λ . There is little sign of an ok developing at this stage, but when α reaches 6° it is quite pronounced, extending back to $\xi = 0.31$ at $\theta = 110^\circ$. There is some uncertainty at the tip of the ok but elsewhere we are confident that the separation line defines the limit λ_A of the region of accessibility since the streamlines on the normals to λ_S either touch this surface or are directed out of it i.e. away from 0. The region of cross-flow reversal extends further towards the nose and the phenomenon becomes stronger so that the characteristic box is essential if the whole region upstream of λ_A is to be computed. On the windward side cross-flow reversal is soon followed by separation and a careful study of the natures of the solution near λ_S supports the view that it is singular at λ_S as described by Brown. This irregularity is best seen in the

behavior of E_∞ (Fig. 5c) which is clearly infinite at separation. On the leeward side the structure is more obscure but the limiting streamlines appear to have to turn until they are almost pointing in the opposite direction to those of external streamlines above them. The structure of the neighborhood of the ok is very certain but what evidence there is suggests that ℓ_A is smooth and continuous there. At the ok the direction of the external streamline is unfavorable on the leeward side and so according to Fig. 7b there may well be a small length of ℓ_A not coincident with ℓ_S , which is then uncomputable.

At $\alpha = 15^\circ$ and 30° the windward part of ℓ_S is very close to the cross-flow reversal but there seems little doubt that ℓ_S is an envelope of limiting streamlines, the most convincing evidence coming from the behavior of E_∞ . The singularity in E_∞ is strongest at the tip of the ok and on the leeward side the solution breaks down almost exactly on the external streamline through this point. No difficulty at all is experienced in integrating the equations from ℓ provided the characteristic box is used so long as we are upstream of this line. Here however, and quite suddenly, convergence of p, q is lost at the outer edge of the boundary layer as would be expected since the corresponding external streamline is carrying the data of its numerical singularity at the ok with it. Thus the limit ℓ_A of the accessible region on the leeward side is not provided by ℓ_S but by the external streamline through the ok. Not only have we failed to compute the leeward side of ℓ_S but we may firmly state that it is uncomputable — and indeed has no meaning for the problem originally posed.

Previously several authors, notably Wang (1974) and Geissler (1976) have attempted to compute the flow pattern in a region of moderate or strong cross-flow reversals but all have soon experienced considerable difficulties due to

deficiencies in their computational procedure. Wang's calculations are probably the most successful but for $\alpha = 30^\circ$ $b/a = 1/4$ he is hardly able to proceed past $\xi = -0.88$ for $\theta \geq 150^\circ$ the line of zero cross-flow crossing λ at $\xi \simeq 0.92$. Using his knowledge of the experimental information about the laminar boundary layer on prolate spheroid, Wang infers that the leeside of λ_s coincides with the windward side of λ_s at least as far as $\xi = -0.4$ and that this is an example of open separation. Our studies show that such a claim is not legitimate for it is quite impossible to integrate the equations on the leeward side far enough towards the windward side to reach λ_s . The concept of 'open' separation has no place whatsoever in the theory of three dimensional boundary layers on prolate spheroids when the pressure gradient is prescribed once it is found a singularity occurs at the ok of accessibility.

There are cogent reasons for believing that open separation is an important feature of experiments on flow past thin spheroids at high Reynolds number. In addition to that adduced by Wang, further evidence may be seen in the beautiful experiments recently reported by Han and Patel (1979). However in all these examples the external velocity field is not determined by inviscid arguments only but also involves a subtle interplay with the boundary layer. An immediate consequence is that the singularity at λ_s on the windward side is prevented and from that it follows that λ_s cannot be an envelope of limiting streamlines. Thus for a real flow Lighthill's concept (1963) of λ_s as a limiting streamline is relevant. Integration of the equations across λ_s may well be possible and if it is an example of open separation we should be able to continue all the way to λ ($\theta = 180^\circ$). On the other hand if λ_s is closed, a good approximate

result might well be obtained if a variation of the Reyhner-Flügge-Lotz (1968) approach were used. If a more accurate answer were required, there are methods in two dimensions available for making use of downstream conditions (Williams, 1975, Cebeci, Keller and Williams, 1979) which seem capable of generalization.

VI. REFERENCES

- Banks, W.H.H. (1976) The Laminar Boundary Layer on a Rotating Sphere, *Acta Mechanica* 24, 273-287.
- Brown, S.N. (1965) Singularities Associated with Separating Boundary Layers, *Phil. Trans. Roy. Soc. London A* 257, 409-444.
- Buckmaster, J. (1972) Perturbation Techniques for the Study of Three-dimensional Separation, *The Physics of Fluids* 15, 2106-2173.
- Burggraf, O.R. (1978) Private communication.
- Cebeci, T. (1979) The Laminar Boundary Layer on a Circular Cylinder Started Impulsively From Rest. *J. Comp. Phys.* 31, pp. 153-172.
- Cebeci, T. and Bradshaw, P. (1977) Momentum Transfer in Boundary Layers, McGraw-Hill/Hemisphere Publishing Co., Washington.
- Cebeci, T., Chang, K.C. and Kaups, K. (1978) A General Method for Calculating Three-Dimensional Laminar and Turbulent Boundary Layers on Ships Hulls, *Proc. 12th Symp. on Naval Hydrodynamics*, Washington, 188-208.
- Cebeci, T., Hirsh, R.S. and Kaups, K. (1976) Calculation of Three Dimensional Boundary Layers on Bodies of Revolution at Incidence, Rept. MDC J7643, Douglas Aircraft Co., Long Beach.
- Cebeci, T., Kaups, K., Mosinskis, G.J. and Rehn, J.A. (1973) Some Problems of the Calculation of Three-Dimensional Boundary-Layer Flows on General Configuration, NASA CR-2285, Washington.
- Cebeci, T., Keller, H.B. and Williams, P.G. (1979) Separating Boundary-Layer Flow Calculations, *J. Comp. Phys.* 31, 363-378.
- Cebeci, T., Khattab, A.K. and Stewartson, K. (1980) On Nose Separation, *J. Fluid Mech.* (to be published).
- Cebeci, T. and Stewartson K. (1977) Unpublished work.
- Eichelbrenner, E.A. and Oudart, A. (1955) *Méthode de Calcul de la Couche Limite Tridimensionnelle, Application á un Corps Fuselé Incliné sur le Vent*, ONERA Publication 76, Paris, France.
- Eichelbrenner, E.A. (1973) Three-Dimensional Boundary Layers, in *Annual Review of Fluid Mechanics*, 5, 339-360.

- Geissler, W. (1975) Calculation of the Three-Dimensional Laminar Boundary Layer Around Bodies of Revolution at Incidence and With Separation, AGARD CP-168.
- Goldstein, S. (1972) On Boundary-Layer Flow Near a Position of Separation, Quart. J. Mech. and Appl. Math. 1, 43-69.
- Han Taeyoung and Patel, V.C. (1979) Flow Separation on a Spheroid at Incidence, J. Fluid Mech. 92, 643-657.
- Hayes, W.D. (1951) The Three-Dimensional Boundary Layer, Rept. U.S. Nav. Ord. Lab. No. 13 13.
- Hirsh, R.S. and Cebeci, T. (1977) Calculation of Three-Dimensional Boundary Layers with Negative Cross-Flow On Bodies of Revolution, AIAA Paper 77-683.
- Howarth, L. (1951) The Boundary Layer in Three-Dimensional Flow, Part II: The Flow Near a Stagnation Point, Phil. Mag. (7) 42, 1433-40.
- Krause, E., Hirschel, E.H. and Bothmann, Th. (1968) Die Numerische Integration der Bewegungs-Gleichungen Dreidimensionalen Laminaren Kompressiblen Grenzschichten, Band 3, FACHTAGUNG Aerodynamik, Berlin; DGLR-Fachlinchreihe.
- Lighthill, M.J. (1963) Laminar Boundary Layers, Ed. by L. Rosenhead, Oxford University Press, Oxford, England.
- Maskell, E.C. (1955) Flow Separation in Three Dimensions, RAE Rept. Aero 2565, Royal Aircraft Establishment, Bedford, England.
- Meier, H.U. and Kreplin, H.P. (1979) Experimental Investigation of the Transition and Separation Phenomena on a Body of Revolution, Turbulent Shear Flow Symposium, London.
- Patel, V.C. and Choi, W. (1979) Calculation of Three-Dimensional and Turbulent Boundary Layers on Bodies of Revolution at Incidence, Turbulent Shear Flow Symposium, London.
- Raetz, G.S. (1957) A Method of Calculating Three-Dimensional Laminar Boundary Layers of Steady Compressible Flows, Rept. No. NAI 58-73, Northrop Corp.
- Reyhner, T. A. and Flüge-Lotz, I. (1968) The Interaction of a Shock-Wave with a Laminar Boundary Layer, Int. J. Nonlinear Mech., 3 173-199.
- Smith, F.T. (1977a) The Laminar Separation of an Incompressible Fluid Streaming Past a Smooth Surface, Proc. Roy. Soc. London A 356, 443-464.

- Smith, F.T. (1977b) Behavior of a Vortex Sheet Separating From a Smooth Surface, RAE Tech. Rept. TR 77058.
- Smith, F.T. (1979) Laminar Flow of an Incompressible Fluid Past a Blunt Body; the Separation, Reattachment, Eddy Properties and Drag, J. Fluid Mech., 92, 171-205.
- Smith, F.T., Sykes, R.I. and Brighton, P.W.M. (1977) A Two-Dimensional Boundary Layer Encountering a Three-Dimensional Hump, J. Fluid Mech., 83, 163-176.
- Stewartson, K., Cebeci, T. and Chang, K.C. (1980) A Boundary-Layer Collision in a Curved Duct. To appear in Quart. J. Mech. and Appl. Math.
- Sychev, V. Ya. (1967) On Laminar Flow Behind a Blunt Body at High Reynolds Numbers, Rept. to 8th Symposium on Recent Problems in Mech. Liquids and Gases, Tardo, Poland.
- Sychev, V. Ya. (1972) Concerning Laminar Separation, Izv. Akad. Nauk SSSR Mekh. Zh. Gaza, 3, 47.
- Sykes, R.I. (1979) Ph.D. Thesis, London Univ., London, England.
- Wang, K.C. (1970) Three-Dimensional Boundary Layer Near the Plane of Symmetry of a Spheroid at Incidence, J. Fluid Mech., 43, 187-209.
- Wang, K.C. (1972) Separation Patterns of Boundary Layer Over an Inclined Body of Revolution, AIAA J., 10, 1044-1050.
- Wang, K.C. (1974a) Boundary Layer Over a Blunt Body at High Incidence with an Open-Type of Separation, Proc. Royal Soc., London A 340, 33-55.
- Wang, K.C. (1974b) Laminar Boundary Layer Near the Symmetry-Plane of a Prolate Spheroid, AIAA J., 12, 949-958.
- Wang, K.C. (1974c) Boundary Layer Over a Blunt Body at Extremely High Incidence, The Physics of Fluids, 17, 1381-1385.
- Wang, K.C. (1975) Boundary Layer Over a Blunt Body at Low Incidence with Circumferential Reversed Flow, J. of Fluid Mech., 72, 49-65.
- Wang, K.C. (1976) Separation of Three-Dimensional Flow; in Viscous Flow Symposium, Lockheed Georgia Co., Atlanta, Georgia.
- Williams, P.G. (1975) A Reversed-Flow Computation in the Theory of Self-Induced Separation, Proc. 4th Int. Conf. on Num. Math. in Fluid Dynamics (ed. R.D. Richtmyer) Lecture Notes in Physics, 35, 445-451.

UNCLASSIFIED

SECURITY CLASSIFICATION OF THIS PAGE (When Data Entered)

REPORT DOCUMENTATION PAGE		READ INSTRUCTIONS BEFORE COMPLETING FORM	
1. REPORT NUMBER MDC-J8716	2. GOVT ACCESSION NO. AD-A085159	3. RECIPIENT'S CATALOG NUMBER (9)	
4. TITLE (and Subtitle) STUDIES ON THREE-DIMENSIONAL BOUNDARY LAYERS ON BODIES OF REVOLUTION. II. THREE-DIMENSIONAL LAMINAR BOUNDARY LAYERS AND THE OK OF ACCESSIBILITY		5. TYPE OF REPORT FINAL rept.	15 Sep 78 - 15 Dec 79
6. AUTHOR Tuncer/Cebeci A. A./Khatab Keith/Stewartson		7. CONTRACT OR GRANT NUMBER(s) N61921-78-C-0158/ew	
8. PERFORMING ORGANIZATION NAME AND ADDRESS McDonnell Douglas Corporation Douglas Aircraft Company 3855 Lakewood Blvd. Long Beach, CA 90846		10. PROGRAM ELEMENT, PROJECT, TASK AREA & WORK UNIT NUMBERS 61153N:WR023-02; WR023 02 003 CA82AA	
11. CONTROLLING OFFICE NAME AND ADDRESS Naval Air Systems Command (AIR 320C) Washington, D.C. 20361		12. REPORT DATE Apr 1980	
14. MONITORING AGENCY NAME & ADDRESS (if different from Controlling Office) Naval Surface Weapons Center (R44) Silver Spring, MD 20910		13. NUMBER OF PAGES 65	
		15. SECURITY CLASS. (of this report) Unclassified	
		15a. DECLASSIFICATION/DOWNGRADING SCHEDULE	
16. DISTRIBUTION STATEMENT (of this Report) Approved for public release; distribution unlimited			
17. DISTRIBUTION STATEMENT (of the abstract entered in Block 20, if different from Report) (16) WR 023 02			
18. SUPPLEMENTARY NOTES (12) 66			
19. KEY WORDS (Continue on reverse side if necessary and identify by block number) Boundary Layers Laminar Boundary Layers Boundary-Layer Separation Three-Dimensional Boundary Layers Prolate Spheroid			
20. ABSTRACT (Continue on reverse side if necessary and identify by block number) An investigation is carried out into the structure of the laminar boundary layer originating from the forward stagnation point of a prolate spheroid at incidence in a uniform stream, assuming that the external velocity distribution is given by attached potential theory. The principal new results of the study are: (1) A new transformation of the body coordinates is devised which facilitates the computation of the solution near the nose.			

DD FORM 1473
1 JAN 73EDITION OF 1 NOV 68 IS OBSOLETE
S/N 0102-014-6601

UNCLASSIFIED

SECURITY CLASSIFICATION OF THIS PAGE (When Data Entered)

116400

Lun

UNCLASSIFIED

SECURITY CLASSIFICATION OF THIS PAGE(When Data Entered)

(ii) Two variations of the standard box method of solving the equations are devised to enable solutions to be computed in regions of cross-flow reversal.

(iii) Whereas in two-dimensional flows the effect of the boundary layer approaching separation on the external flow may be represented by a blowing velocity, in the present study we find that this is only true near the windward line of symmetry. Near the leeward line of symmetry the blowing velocity must be replaced by a suction velocity even though the boundary layer is being significantly thickened.

(iv) The boundary layer over the whole of the spheroid cannot be computed in an integration from the forward stagnation point.

UNCLASSIFIED

SECURITY CLASSIFICATION OF THIS PAGE(When Data Entered)